

Integrability of Generalised Skew-Symmetric Replicator Equations via Graph Embeddings

Matthew Visomirski¹ and Christopher Griffin²

¹Department of Physics, The Pennsylvania State University, University Park, PA 16802

²Applied Research Laboratory, The Pennsylvania State University, University Park, PA 16802

E-mail: mav5583@psu.edu, griffinch@psu.edu

Abstract. It is known that there is a one-to-one mapping between oriented directed graphs and zero-sum replicator dynamics (Lotka-Volterra equations) and that furthermore these dynamics are Hamiltonian in an appropriately defined nonlinear Poisson bracket. In this paper, we investigate the problem of determining whether these dynamics are Liouville-Arnold integrable, building on prior work graph in graph decloning by Evripidou et al. [J. Phys. A., 55:325201, 2022] and graph embedding by Paik and Griffin [Phys. Rev. E. 107(5): L052202, 2024]. Using the embedding procedure from Paik and Griffin, we show (with certain caveats) that when a graph producing integrable dynamics is embedded in another graph producing integrable dynamics, the resulting graph structure also produces integrable dynamics. We also construct a new family of graph structures that produces integrable dynamics that does not arise either from embeddings or decloning. We use these results to classify the dynamics generated by almost all oriented directed graphs on six vertices, with three hold-out graphs that generate integrable dynamics and are not part of a natural taxonomy arising from known families and graph operations. These hold-out graphs suggest more structure is available to be found. Moreover, the work suggests that oriented directed graphs leading to integrable dynamics may be classifiable in an analogous way to the classification of finite simple groups, creating the possibility that there is a deep connection between integrable dynamics and combinatorial structures in graphs.

Keywords: integrable system, replicator equation, Lotka-Volterra equation, graphs

1. Introduction

Conserved quantities are fundamental in both classical and modern physics with the correspondence between continuous symmetries and conserved quantities given by Noether's theorem [1], providing a theoretical foundation for many of our theories [2, 3]. Dynamical systems exhibiting a sufficient number of conserved quantities (and generated by an appropriate Poisson bracket) are Liouville-Arnold integrable, admitting solutions that trace out foliating tori in phase space [4]. Integrable systems are rare, in the sense that a randomly chosen system of differential equations is unlikely to be Hamiltonian, let alone integrable. In light of Smale's comments and analysis [5], it is surprising to find large families of integrable dynamics appearing in evolutionary dynamics, yet it is known that there are classes of Lotka-Volterra dynamics that are integrable in the Liouville-Arnold sense (see [6–11] for examples).

Let $\mathbf{A} \in \mathbb{R}^{n \times n}$ be a payoff (interaction) matrix. The replicator dynamics [12, 13] are the system of differential equations with form,

$$\dot{x}_i = x_i (\mathbf{e}_i^T \mathbf{A} \mathbf{x} - \mathbf{x}^T \mathbf{A} \mathbf{x}),$$

where $\mathbf{x} = \langle x_1, \dots, x_n \rangle$ is a vector of species proportions and \mathbf{e}_i is the i^{th} standard basis vector. As such $\mathbf{x} \in \Delta_{n-1}$, where,

$$\Delta_{n-1} = \left\{ \mathbf{x} \in \mathbb{R}^n : \sum_i x_i = 1, x_i \geq 0 \right\},$$

is the $n-1$ dimensional unit simplex embedded in \mathbb{R}^n . In a game-theoretic interpretation, \mathbf{A} is a payoff (reward) matrix resulting from the interaction of two species; i.e., playing a game. See Hofbauer and Sigmund or [12, 13], Weibull [14] or Tanimoto [15, 16] for a complete introduction to evolutionary games, and the replicator dynamics.

It is well known that the replicator dynamics are diffeomorphic to the generalised Lotka-Volterra equations [12, 13]. In the special case that \mathbf{A} is skew-symmetric, the replicator equations simplify to,

$$\dot{x}_i = x_i (\mathbf{e}_i^T \mathbf{A} \mathbf{x}), \tag{1}$$

and in this case, we have an instance of the Lotka-Volterra equations with no need for a specialised diffeomorphism [10]. This class of evolutionary games models two-player, zero-sum games like rock-paper-scissors and was originally studied by Akin and Losert [17]. Interestingly, this class of model is used extensively in theoretical ecology [18–20] when the entries of \mathbf{A} are restricted to $0, \pm 1$. Surprisingly, these models also find use in theoretical physics, with these dynamics occurring in the analysis of Schrödinger operator [21] in the work by Veselov and Shabat and in the discrete Korteweg-De Vries (KdV) equation (the Volterra lattice) as analysed by Moser [22] and Kac and Moerbeke [23], with generalisations by Bogoyavlensky [24].

Any skew-symmetric matrix \mathbf{A} can be represented as an oriented directed graph $G_{\mathbf{A}} = (V, E)$, where $V = \{1, \dots, n\}$ and there is a directed edge $(i, j) \in E \subset V \times V$

precisely when $\mathbf{A}_{ij} < 0$ with corresponding weight A_{ji} . From a high-level ecological perspective, this interpretation is most sensible when we restrict the entries of \mathbf{A} to $0, \pm 1$ and in this case, we have $A_{ij} = -1$ precisely when species j preys on species i as represented by the directed edge (i, j) in $G_{\mathbf{A}}$. As a consequence of the mappings between the graph $G_{\mathbf{A}}$, the skew-symmetric matrix \mathbf{A} and the replicator (Lotka-Volterra) dynamics given in Eq. (1), we say that a graph $G_{\mathbf{A}}$ is (Liouville-Arnold) integrable if and only if the corresponding (Liouville-Arnold) dynamical system is integrable.

In this paper, we restrict our attention to the (partial) integrability of the replicator (Lotka-Volterra) dynamics arising from the case when the matrix \mathbf{A} is both skew-symmetric and has entries 0 or ± 1 . In this work, we build on and use the prior work of Itoh [6, 7], Bogoyavlenskij, Itoh and Yukawa [8] and Evripidou, Kassotakis and Vanhaecke [9, 10] and Griffin and Paik [11] who along with others, have done extensive work on this class of systems [25, 26]. The main results of this paper, which we make precise in the sequel, are as follows.

- (i) We characterise a new infinite family of integrable graphs that we call the *skip vertex graphs*. This extends the work of Bogoyavlenskij [8, 24] and hints at a potentially more general theory of integrability for these systems.
- (ii) We show under certain conditions, if an inner graph G_{in} is embedded in an outer graph G_{out} and both graphs are integrable, then the resulting graph is integrable. We generalise this result to multiple simultaneous embeddings, defining the concept of an embedding graph.
- (iii) Using these results, as well as the results on graph morphisms developed by Evripidou et al. [10], we characterise the behaviour of all replicator (Lotka-Volterra) dynamics generated by directed graphs up to six vertices. Interestingly, there are still three “hold-out” graphs that produce integrable dynamics, but are not members of the integrable families we discuss, suggesting a more complete characterisation is needed.

This paper represents another step toward the ultimate goal of characterising the (zero-sum) replicator dynamics generated from directed graphs as a function of the graph structures themselves, largely begun with the early work on the Volterra lattice [22, 23]. Our ultimate goal is to characterise the combinatorial [6, 7] structures that lead to integrable (or partially integrable) dynamics, and thus to provide a new and potentially deep connection between combinatorics and dynamics.

The remainder of this paper is organised as follows: In Section 2, we provide preliminary definitions and results from prior work (e.g., [6, 10, 11, 24]) that will be used throughout the rest of the paper. We present our main results on graph embeddings in Section 4 and the new class of integrable graphs in Section 3. Using these results, we provide the taxonomy of the dynamics arising from graphs containing up to six vertices in Section 6. Conclusions and future directions of research are presented in Section 7. Mathematica notebooks containing code that assisted us in developing these results are provided as supplemental material.

2. Preliminary Definitions and Results

We provide mathematical preliminaries, most of which can be found in Evripidou et al. [10] and Paik and Griffin [11]. Material on Poisson structures is provided in detail in Laurent-Gengoux, Pichereau and Vanhaecke's book on the subject [4]. For brevity, we omit most details and refer the interested reader to the appropriate references.

2.1. Graph Operations

We formalise the one-to-one relationship between directed graph structures and skew-symmetric matrices with entries restricted to $0, \pm 1$. For this, recall that a directed graph $G = (V, E)$ is oriented the edge (i, j) either does not appear in E or if it does appear, then the edge (j, i) does not appear in E . The following definition is adapted from Evripidou et al. [10].

Definition 2.1 (Skew Symmetric Graph). Let $\mathbf{A} \in \mathbb{R}^{n \times n}$ be a skew-symmetric matrix with entries consisting of only 0 and ± 1 . The oriented directed graph $\mathbf{G}_{\mathbf{A}} = (V, E)$ has vertex set $V = \{1, \dots, n\}$ and edge set $E \subset V \times V$ so that,

$$(i, j) \in E \iff A_{ij} = -1.$$

The following relationship is easy to see.

Proposition 2.2. *There is a one-to-one correspondence between oriented directed graphs and skew-symmetric matrices with entries $0, \pm 1$.* \square

Evripidou et al. [10] refer to this class of graphs as skew-symmetric graphs. For the remainder of this paper, all graphs will be skew-symmetric and will just be called graphs.

Definition 2.3 (Graph Embedding). Let $G_{\text{in}} = (V_{\text{in}}, E_{\text{in}})$ and $G_{\text{out}} = (V_{\text{out}}, E_{\text{out}})$ two graphs with disjoint vertex sets and suppose v is a vertex in G_{out} . Let $\tilde{E}_{\text{out}} \subset E_{\text{out}}$ be the set of edges in E_{out} not containing v . The embedding graph $J = G_{\text{in}} \hookrightarrow_v G_{\text{out}}$ has vertex set $V = V_{\text{in}} \sqcup (V_{\text{out}} \setminus \{v\})$ and edge set $E = E_{\text{in}} \sqcup \tilde{E}_{\text{out}} \sqcup E_{\text{embed}}$, where,

$$(i, j) \in E_{\text{embed}} \iff (i \in V_{\text{in}} \wedge j \in V_{\text{out}} \wedge (v, j) \in E_{\text{out}}) \vee (i \in V_{\text{out}} \wedge j \in V_{\text{in}} \wedge (i, v) \in E_{\text{out}}).$$

The process of graph embedding is illustrated in Fig. 1 and was suggested by Paik (in [11]) and inspired by Curto et al.'s cyclic union [27, 28]. Notice we are embedding into vertex 1 of G_{out} . In the resulting graph, we decorate the vertices remaining from G_{out} with tildes. Let $\mathbf{A}_{\text{in}} \in \mathbb{R}^{n_{\text{in}} \times n_{\text{in}}}$ be the skew-symmetric matrix corresponding to G_{in} and let $\mathbf{A}_{\text{out}} \in \mathbb{R}^{n_{\text{out}} \times n_{\text{out}}}$ be the skew-symmetric matrix corresponding to G_{out} . Let,

$$\mathbf{A}_{\text{out}} = \begin{bmatrix} 0 & \mathbf{r}^T \\ -\mathbf{r} & \tilde{\mathbf{A}}_{\text{out}} \end{bmatrix}, \quad (2)$$

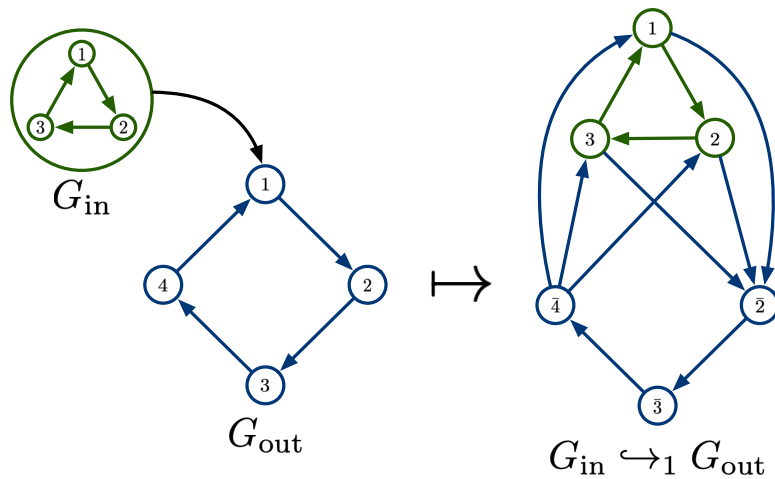


Figure 1. The directed three-cycle is embedded into a directed four-cycle. The edges in the three cycle are preserved. The edges in the four-cycle to and from the replaced vertex are replicated to each vertex in the embedded three-cycle. The remaining vertices from the four-cycle are adorned with bars.

where \mathbf{r}^T is an appropriately sized row vector. Suppose we embed G_{in} into the vertex corresponding to the first row (column) of \mathbf{A}_{out} . That is, let $v = 1$ in Definition 2.3. Then the skew-symmetric matrix for the graph embedding is given by,

$$\mathbf{A} = \begin{bmatrix} \mathbf{A}_{\text{in}} & \mathbf{R}^T \\ -\mathbf{R} & \tilde{\mathbf{A}}_{\text{out}} \end{bmatrix}, \quad (3)$$

with,

$$\mathbf{R} = \begin{bmatrix} \mathbf{r} & \mathbf{r} & \cdots & \mathbf{r} \end{bmatrix}, \quad (4)$$

having n_{in} columns all equal to \mathbf{r} . We will use this construction in the proof of Theorem 4.2.

The following operation is defined by Evripidou et al. [10] and will be used in our classification of dynamics arising from graphs with at most six vertices.

Definition 2.4 (Cloned Vertices). Suppose $G_{\mathbf{A}} = (V, E)$ is a graph corresponding to the matrix \mathbf{A} . A vertex $j \in V$ is a clone of $i \in V$ if j and i share the same neighbourhood in G . Equivalently, if row i of \mathbf{A} and row j of \mathbf{A} are identical, then i and j are clones.

Definition 2.5 (Irreducible Graph). A graph $G_{\mathbf{A}}$ is irreducible if $G_{\mathbf{A}}$ has no cloned vertices or equivalently if each row of \mathbf{A} is unique.

If a graph $G_{\mathbf{A}} = (V, E)$ has cloned vertices, then it is straightforward to see we can partition V into subsets V_1, \dots, V_n for some $n \geq 1$, where if $i, j \in V_k$, then i and j are clones. Since the vertices in V_k share neighbourhoods, we can map $G_{\mathbf{A}}$ to a new irreducible graph $\tilde{G}_{\tilde{\mathbf{A}}} = (\tilde{V}, \tilde{E})$ with $\tilde{V} = \{1, \dots, n\}$ and $(i, j) \in \tilde{E}$ if and only if there is some $v \in V_i$ and $w \in V_j$ so that $(v, w) \in E$. It is straightforward to see that the new skew-symmetric matrix $\tilde{\mathbf{A}}$ is simply the matrix \mathbf{A} with duplicate rows and their corresponding columns removed.

Definition 2.6 (Decloning). Let $G_{\mathbf{A}}$ be a graph. The mapping $\eta : G_{\mathbf{A}} \mapsto \tilde{G}_A$ is the decloning operation.

Fig. 2 shows a 5 vertex graph on the left in which vertices 3, 4 and 5 are clones. The decloned form of the graph is shown on the right. The decloning construction will

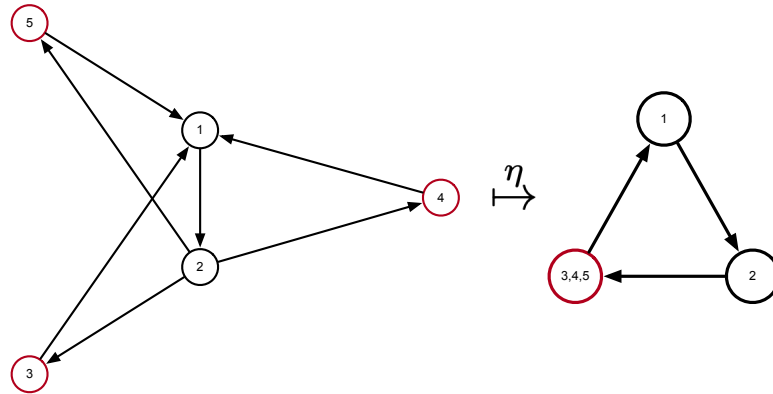


Figure 2. An example of decloning a graph.

be used as part of our classification scheme for the dynamics generated by graphs with fewer than 7 vertices.

We will frequently refer to a special class of graphs, sometimes referred to as Bogoyavlenskij -Itoh graphs, or sometimes just the Bogoyavlenskij graphs [10].

Definition 2.7 (Bogoyavlenskij Graphs). The *Bogoyavlenskij graph* $B(n, k)$ where $k < \frac{n}{2}$ has vertex set $V = \{1, \dots, n\}$ and edge E with edge $(i, j) \in E$ if $j = 1 + (i \oplus_n l)$ for $0 \leq l < k$, where \oplus_n denotes addition modulo n .

Put more simply, if we arrange the numbers in $\{1, \dots, n\}$ in a circle, then the graph $B(n, k)$ has edges from vertex i to the next k vertices working around the circle. This is illustrated in Fig. 3.

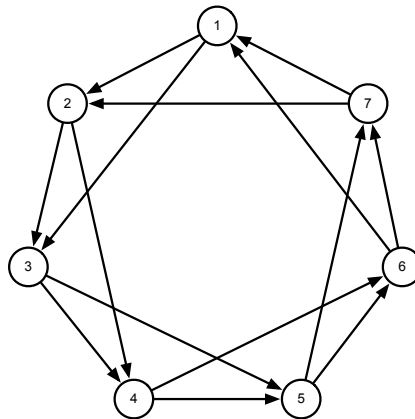


Figure 3. The Bogoyavlenskij graph $B(7, 2)$ illustrates the definition of these graphs using geometric arrangement.

2.2. Integrability of Replicator Systems

Let $\mathbf{A} \in \mathbb{R}^{n \times n}$ be a skew-symmetric matrix and let $F, G : \mathbb{R}^n \rightarrow \mathbb{R}$ be differentiable functions. Define the bracket,

$$\{F, G\}_{\mathbf{A}} = \sum_{i < j} A_{ij} x_i x_j \left(\frac{\partial F}{\partial x_i} \frac{\partial G}{\partial x_j} - \frac{\partial G}{\partial x_i} \frac{\partial F}{\partial x_j} \right). \quad (5)$$

Direct computation shows that Eq. (1) is a Hamiltonian system with Hamiltonian $H_1(\mathbf{x}) = x_1 + \dots + x_n$. That is, Eq. (1) can be rewritten as,

$$\dot{x}_i = \{x_i, H_1\}_{\mathbf{A}}.$$

and H_0 is a conserved quantity, i.e., $\dot{H}_1 = 0$, which is obvious for the replicator as we automatically have $H_1 = 1$, assuming we begin with an initial condition on Δ_{n-1} . It is known that certain instances of the replicator (Lotka-Volterra) dynamics admit additional conserved quantities [6, 7, 11], which we will discuss in the sequel. As an interesting historical note, the nonlinear (quadratic) bracket defined in Eq. (5) is not well known in the broader literature and has been used and/or “rediscovered” on several occasions including (for example) by Itoh [6], Griffin [29], Ovsienko, Schwartz and Tabachnikov [30], even though it does appear in textbooks by Marsden and Ratiu [31] and Laurent-Gengoux, Pichereau and Vanhaecke [4].

The Poisson structure corresponding to this bracket,

$$\pi_{\mathbf{A}} = \sum_{i < j} A_{ij} x_i x_j \frac{\partial}{\partial x_i} \wedge \frac{\partial}{\partial x_j},$$

has been studied extensively by Evripidou et al. [10] and is discussed in [4]. In particular, the dimension of $\pi_{\mathbf{A}}$ precisely corresponds to the rank of \mathbf{A} . The following definition follows immediately from this fact and Def. 12.9 of [4].

Definition 2.8. Let $\mathbf{A} \in \mathbb{R}^{n \times n}$ be a skew-symmetric matrix with rank denoted $\text{rank}(\mathbf{A})$. The replicator (Lotka-Volterra) dynamics, Eq. (1), generated from \mathbf{A} are *integrable* if there are s conserved quantities H_1, \dots, H_s so that:

- (i) H_1, \dots, H_s are (algebraically) independent.
- (ii) H_1, \dots, H_s are in involution, or commute under the bracket. That is, $\{H_i, H_j\}_{\mathbf{A}} = 0$ for all i, j .
- (iii) The following relation among matrix rank (Poisson manifold dimension), embedding dimension and number of conserved quantities holds,

$$s + \frac{1}{2} \text{Rank}(\mathbf{A}) = n.$$

As noted in [10], the Casimirs of the Poisson algebra corresponding to $\pi_{\mathbf{A}}$ can be read from the eigenvectors of \mathbf{A} corresponding to the zero eigenvalue. To see this, note that if $\boldsymbol{\alpha} = \langle \alpha_1, \dots, \alpha_n \rangle$ is an eigenvector of \mathbf{A} with eigenvalue 0, then,

$$\frac{d}{dt} (x_1^{\alpha_1} \dots x_n^{\alpha_n}) = x_1^{\alpha_1} \dots x_n^{\alpha_n} (\boldsymbol{\alpha}^T \mathbf{A} \mathbf{x}) = 0, \quad (6)$$

and thus $x_1^{\alpha_1} \cdots x_n^{\alpha_n}$ is a conserved quantity of the system. It is worth noting that Akin and Losert's [17] noted that these quantities were conserved in the context of zero-sum replicator dynamics, but studied them purely from the perspective of symplectic geometry in which they were treated as the Hamiltonians. In unrelated work, Hamiltonian structure in evolutionary games was also considered by Hofbauer [32]. Neither Hofbauer nor Akin and Losert consider general integrability.

In general, there will be more conserved quantities than just the Casimirs, as shown in special cases by Kac and Moser [23] and Moerbeke [22], Bogoyavlenskij [8, 33] and especially by Itoh [6, 7], who provided a combinatorial analysis to the construction of conserved quantities in Bogoyavlenskij graphs. In particular, the following theorem is immediate from the work of Itoh and Bogoyavlenskij [6–8].

Theorem 2.9. *Let $G = B(n, k)$ be a Bogoyavlenskij graph. Then G is integrable. \square*

Itoh's combinatorial description [7] of the conserved quantities can be rephrased using graph theoretic language. We do so for the class $B(n, 1)$, which is equivalent to the class of directed cycles, as we will use these conserved quantities later in discussing a new family of integrable graphs.

Consider the directed cycle with n vertices (see G_{in} or G_{out} in Fig. 1). Evripidou et al. [10] refer to this as $\text{KM}(n) \equiv B(n, 1)$ for the work of Kac and van Moerbeke [23] and Moser [22] whose work on the Volterra lattice predates the work of Kac and van Moerbeke. For reasons that will be clear in the sequel, let,

$$s = \left\lfloor \frac{n}{2} \right\rfloor + 1.$$

In the dynamical system generated from the graph, $\text{KM}(n)$, there are always two conserved quantities,

$$H_1 = \sum_i x_i \quad \text{and} \quad H_s = \prod_i x_i.$$

We note that the corresponding game (interaction) matrix has rank $n - 2$ when n is even and rank $n - 1$ when n is odd. Consequently, when n is odd, there will be $\left\lfloor \frac{n}{2} \right\rfloor = \left\lfloor \frac{n}{2} \right\rfloor + 1$ conserved quantities and when n is even, there will be $\frac{n}{2} + 1 = \left\lfloor \frac{n}{2} \right\rfloor + 1$ conserved quantities.

Define a *non-edge* as the pair (i, j) with $i < j$ so that neither (i, j) nor (j, i) is an element of E . Likewise, define a *non-cycle* as a sequence (i_1, \dots, i_r) so that, $i_j < i_{j+1}$, and for all pairs (i_j, i_k) , the pair (i_j, i_k) is a non-edge and the pair (i_1, i_r) is also a non-edge. Thus, (i_1, \dots, i_r) forms a cycle in the graph complement of $\text{KM}(n)$. Denote the set of all non-edges as \overline{E} and the set of all non-cycles of length l as $\overline{\mathcal{C}}(l)$. We can think of non-edges as non-cycles of length 2, that is $\overline{E} = \overline{\mathcal{C}}(2)$. Notice the graph $\text{KM}(n)$ possesses non-empty sets $\overline{\mathcal{C}}(k)$ for $2 \leq k \leq \left\lfloor \frac{n}{2} \right\rfloor$.

Define

$$H_k = \sum_{c \in \overline{\mathcal{C}}(k)} \prod_{j \in c} x_j. \tag{7}$$

The following result follows from [7] and is a restatement of the classical integrability of the Volterra lattice.

Theorem 2.10. *For $1 \leq k \leq s$, the quantity H_k is conserved in the replicator dynamics generated by $\text{KM}(n)$. Moreover, these conserved quantities H_k commute under the nonlinear bracket in Eq. (5).* \square

Both Itoh [6] and Paik and Griffin [11] note that the conserved quantities for odd tournament graphs $B(n, \lfloor \frac{n}{2} \rfloor)$ can be written in terms of sums over products of cycles (rather than non-cycles). For other graphs in $B(n, k)$, the conserved quantities can be expressed as combinations of both sums over products of cycles and non-cycles. Consequently, all conserved quantities can be constructed directly out of the edge structure of $B(n, k)$ or its graph complement. (Details on this generalisation can be found in the supplementary materials.) This observation further supports our goal of characterising the dynamics of the replicator (Lotka-Volterra) equations directly from the graph structures used to generate them.

We require one final, seminal, result proved by Evripidou et al. [10], relating graph decloning and integrability.

Theorem 2.11 (Proposition 4.5 of [10]). *A graph $G_{\mathbf{A}}$ is (super) integrable if and only if its decloned form $\tilde{G}_{\tilde{\mathbf{A}}}$ is integrable.* \square

3. Skip-Vertex Graphs: A New Family of Integrable Graphs

Intuitively, Bogoyavlenskij graphs are cycles with edges added in a way that preserves a notion of rotational symmetry. Here we consider another instance where adding edges to a directed cycle produces another family of integrable graphs, but symmetry is broken.

Definition 3.1 (Skip-Vertex Graph). The skip-vertex graph on $n \geq 4$ vertices with $k \leq \frac{n}{2}$ skips ($k < 2$ for $n = 4$) is (isomorphic to) a graph constructed by adding the edges $(1, 3), (3, 5), \dots, (2k - 1, 2k + 1)$ to the directed cycle with n vertices. We refer to these added edges as *skip-edges* and denote this graph $\text{Sk}(n, k)$. Note when $k = \frac{n}{2}$ addition is modulo n so that the last added edge connects Vertex $n - 1$ to Vertex 1. If the skip-edge $(2k - 1, 2k + 1)$ is present, we call vertex $2k$ a skipped vertex.

The skip-graph $\text{Sk}(8, 3)$ is shown in Fig. 4. The graph $\text{Sk}(n, k)$ has an interaction matrix with the following form,

$$\mathbf{A} = \begin{bmatrix} 0 & -1 & -\alpha_1 & 0 & 0 & \cdots & \alpha_{n-1} & 1 \\ 1 & 0 & -1 & 0 & 0 & \cdots & 0 & 0 \\ \alpha_1 & 1 & 0 & -1 & -\alpha_3 & \cdots & 0 & 0 \\ 0 & 0 & 1 & 0 & 0 & \cdots & 0 & 0 \\ 0 & 0 & \alpha_3 & 0 & 0 & \cdots & 0 & 0 \\ \vdots & \vdots & \vdots & \vdots & \vdots & \ddots & \vdots & \vdots \\ -\alpha_{n-1} & 0 & 0 & 0 & 0 & \cdots & 0 & -1 \\ -1 & 0 & 0 & 0 & 0 & \cdots & 1 & 0 \end{bmatrix}, \quad (8)$$

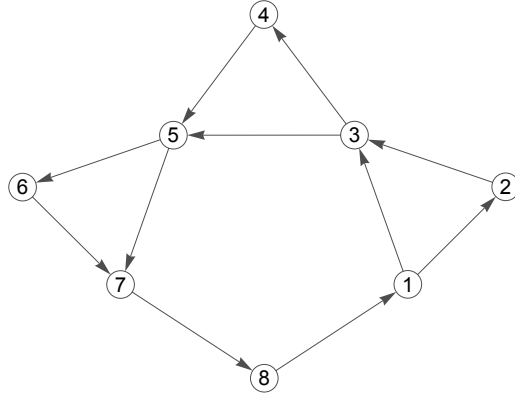


Figure 4. The skip-graph $\text{Sk}(8, 3)$ is shown. Notice this skip-graph is not as symmetric as a graph in the family $B(n, k)$.

where $\alpha_1 = 1$ and by extension, $\alpha_{2i-1} = 1$ if $k \geq i$ and otherwise $\alpha_{2i-1} = 0$.

Lemma 3.2. *The dynamics generated by a skipped-vertex $\text{Sk}(n, k)$ graph has a fixed point in the interior of Δ_{n-1} if and only if n is even.*

Proof. Suppose n is even, and let \mathbf{A} be the interaction matrix from a graph $\text{Sk}(n, k)$. Interior fixed points of Eq. (1) arise from solutions to the equation, $\mathbf{A}\mathbf{x} = \mathbf{0}$, when \mathbf{x} is constrained to lie in the interior of Δ_{n-1} . Thus, it suffices to analyse the eigenvectors of \mathbf{A} corresponding to the zero eigenvalues (and to the Casimirs of the system).

As with the directed cycle with n vertices, \mathbf{A} has two eigenvectors corresponding to zero eigenvalues with form,

$$\mathbf{v}_1 = \begin{bmatrix} 0 \\ 1 \\ 0 \\ 1 \\ \vdots \\ 0 \\ 1 \end{bmatrix} \quad \text{and} \quad \mathbf{v}_2 = \begin{bmatrix} 1 \\ -\alpha_1 \\ 1 \\ -\alpha_3 \\ \vdots \\ 1 \\ 0 \end{bmatrix},$$

with alternating structure. This can be shown by direct computation using Eq. (8). Notice, if $\alpha_{2i-1} = 0$ for all i , then these are the two eigenvectors corresponding to eigenvalue zero in the directed cycle. Let, $\mathbf{v} = \alpha\mathbf{v}_1 + \beta\mathbf{v}_2$, then $\mathbf{A}\mathbf{v} = \mathbf{0}$. We will show there are α and β so that $\mathbf{v} \in \Delta_{n-1}$. If $\mathbf{v} = \langle v_1, \dots, v_n \rangle$, then,

$$\sum_i v_i = \frac{n}{2}\alpha + \left(\frac{n}{2} - k\right)\beta.$$

If $\mathbf{v} \in \Delta_{n-1}$, then we require

$$\frac{n}{2}\alpha + \left(\frac{n}{2} - k\right)\beta = 1,$$

which implies,

$$\beta = \frac{n\alpha - 2}{2k - n}.$$

We also require $\mathbf{v} > 0$. This yields two inequalities,

$$\frac{\alpha n - 2}{n - 2k} > 0 \quad \text{and} \quad \alpha + \frac{\alpha n - 2}{n - 2k} > 0.$$

Using our assumption that $n > 2k$, it follows that we require

$$\frac{1}{n - k} < \alpha < \frac{2}{n},$$

for \mathbf{v} to be a vector in Δ_{n-1} . Thus, the dynamics generated by a graph in $\text{Sk}(n, k)$ have an interior fixed point when n is even.

Now suppose n is odd. As in the case of an odd cycle, the interaction matrix has only one eigenvector with eigenvalue 0. This vector has form,

$$\mathbf{v} = \begin{bmatrix} 1 \\ 1 - \alpha_1 \\ 1 \\ 1 - \alpha_3 \\ 1 \\ \vdots \\ 1 - \alpha_{2k-1} \\ 1 \end{bmatrix}$$

Notice if $\alpha_i = 0$, we recover the unique eigenvector of the interaction matrix of the directed cycle corresponding to the zero eigenvalue, as expected. This vector cannot be scaled to lie in the interior of Δ_{n-1} . Consequently, there is no interior point solution and all solutions asymptotically decay to a lower-order system solution. \square

Consider a skip-graph with $2n$ vertices. Let V_s denote the set of vertices that are not skipped. Notice the eigenvalues in the proof provide two conserved quantities for skip graphs,

$$H_n = x_2 x_4 \cdots x_{2n}$$

$$H_{n+1} = \prod_{i \in V_s} x_i.$$

This can be seen immediately by reading these terms from \mathbf{v}_1 and \mathbf{v} in the proof. For example, these two conserved quantities for the graph shown in Fig. 4, i.e., $\text{Sk}(8, 3)$ are,

$$H_4 = x_2 x_4 x_6 x_8$$

$$H_5 = x_1 x_3 x_5 x_7 x_8.$$

As always, $H_1 = x_1 + x_2 + \cdots + x_{2n}$ is a conserved quantity.

Given the result in Lemma 3.2, we consider only skip-graphs $\text{Sk}(n, k)$ where n is even and use an imagined contrivance of a fluid flowing along the edges of a directed cycle or skip-graph. The fact that the graph is strongly connected implies that this imaginary fluid must circulate through the graph.

Consider the directed cycle $\text{KM}(n)$ with corresponding matrix \mathbf{A}_0 . Consider an arbitrary non-cycle in $\text{KM}(n)$ corresponding to the term $T = x_{i_1} \cdots x_{i_l}$. Then, computing \dot{T} with respect to the dynamics generated by $\text{KM}(n)$ yields,

$$\dot{T} = \left(\prod_{j=1}^n x_{i_j} \right) \left(\sum_{j=1}^n \mathbf{e}_{i_j}^T \right) \mathbf{A}_0 \mathbf{x} = T \cdot (x_{i_{l+1}} - x_{i_{l-1}} + x_{i_{2+1}} - x_{i_{2-1}} + \dots + x_{i_{n+1}} - x_{i_{n-1}}).$$

Addition in the index terms is taken modulo n with appropriate adjustments to count from $1, \dots, n$ if needed. Notice, the sum on the right-hand-side performs in/out flow counting with respect to the non-cycle; i.e., the net sum is composed of terms corresponding to outward flow being negative and inward flow being positive. This is not the case if T contains pairs of variables corresponding to an edge in the graph. Consequently, summing over all these inward and outward flows in non-cycles must yield zero because the graph is strongly connected and flow can only circulate. This is just a restatement of Itoh [7] result.

Now decorate the time derivative operator with the graph used to formulate it. That is,

$$D_{\text{KM}(n)}[T] = \left(\prod_{j=1}^n x_{i_j} \right) \left(\sum_{j=1}^n \mathbf{e}_{i_j}^T \right) \mathbf{A}_0 \mathbf{x} = T \cdot (x_{i_{l+1}} - x_{i_{l-1}} + x_{i_{2+1}} - x_{i_{2-1}} + \dots + x_{i_{n+1}} - x_{i_{n-1}}). \quad (9)$$

Passing to $\text{Sk}(n, k)$, the terms corresponding to non-cycles that do not contain vertices in skip-edges have no change to their time derivative. Now consider a skip-edge of form $(i_j, i_j + 2)$. Say a non-cycle term T contains x_{i_j} (but not x_{i_j+2}). Then,

$$D_{\text{Sk}(n,k)}[T] = D_{\text{KM}(n)}[T] - T x_{i_j+2}.$$

Likewise, if T contains x_{i_j+2} , then,

$$D_{\text{Sk}(n,k)}[T] = D_{\text{KM}(n)}[T] + T x_{i_j+1},$$

This alteration occurs because there may be fluid flow cancellation (both in and out) to the elements of a non-cycle. However, the fact that the time-derivatives of the non-cycles are still counting fluid flow implies that the sum of all non-cycles of a given length will be a conserved quantity because of our imaginary fluid conservation. Thus, we state the following lemma which follows from the discussion above and

Lemma 3.3. Let $\overline{C}_{\text{Sk}(n,k)}(m)$ denote the non-cycles of the skip-graph $\text{Sk}(n,k)$ of length m , and let,

$$H_m = \sum_{c \in \overline{C}_{\text{Sk}(m)}} \prod_{j \in c} x_j.$$

Then H_m is a conserved quantity for $\text{Sk}(n,k)$. \square

Notice that $2 \leq m \leq \frac{n}{2}$. Moreover, non-cycles of length $\frac{n}{2}$ correspond to the eigenvector \mathbf{v}_1 from the proof of Lemma 3.2. Thus, for a skip-graph $\text{Sk}(n,k)$ we have $\frac{n}{2} + 1$ conserved quantities, where n is even. It is worth noting that this explains why conserved quantities are generated from both cycles and non-cycles in graphs in class $B(n,k)$ for large enough k . When there are no non-cycles available to use to create balanced flow, the conserved quantities are written in terms of cycles, which conserve flow differently. This is most obvious in the conserved quantities for balanced tournament graphs (see [6] or [11]).

Using a similar argument, or adapting Itoh's proof technique, we also have the following.

Lemma 3.4. If H_1, \dots, H_{n+1} are the conserved quantities for $\text{Sk}(n,k)$ (where n is assumed to be even), then these quantities commute under the action of the nonlinear bracket in Eq. (5). \square .

Consider a skip graph $G = \text{Sk}(n,k)$ with an even number of vertices n . As noted, this corresponds to an interaction matrix \mathbf{A} with zero eigenvalue having multiplicity two. Consequently, for G to be integrable, we require $\frac{n}{2} + 1$ conserved quantities that commute under the quadratic bracket. We have constructed these conserved quantities.

Theorem 3.5. Let $G = \text{Sk}(n,k)$ for even n and $2k < n$. Then G is integrable. \square

4. Integrability of Graph Embeddings

Given the work by Itoh et al. [6, 7], we now make the following definition.

Definition 4.1. An oriented directed graph G admits Itoh-style conserved quantities if every conserved quantity can be written in the form,

$$H = \sum_{j \in \mathcal{J}} \prod_{i \in \mathcal{I}(j)} x_j, \tag{10}$$

for appropriate index sets $\mathcal{I}(j)$ and \mathcal{J} .

This family necessarily includes all Bogoyavlenskij graphs as well as the skip-vertex graphs.

Theorem 4.2. Let $G_{out} = (V_{out}, E_{out})$ and $G_{in} = (V_{in}, E_{in})$ be two graphs that admit Itoh-style conserved quantities. If $J = G_{in} \hookrightarrow_v G_{out}$, then J is integrable.

Proof. Without loss of generality, we assume $v = 1$ and that G_{out} has n_{out} vertices and G_{in} has n_{in} vertices. Denote the interaction matrices of the graphs by \mathbf{A}_{out} and \mathbf{A}_{in} , respectively. The interaction matrix of J is given by Eq. (3) as,

$$\mathbf{A} = \begin{bmatrix} \mathbf{A}_{\text{in}} & \mathbf{R}^T \\ -\mathbf{R} & \tilde{\mathbf{A}}_{\text{out}} \end{bmatrix}.$$

Define the variables vectors,

$$\begin{aligned} \mathbf{x}_{\text{in}} &= \langle x_1, \dots, x_{n_{\text{in}}} \rangle, \\ \mathbf{x}_{\text{out}} &= \langle x_{\bar{1}}, \dots, x_{\bar{n}_{\text{out}}} \rangle, \quad \text{and} \\ \tilde{\mathbf{x}}_{\text{out}} &= \langle x_{\bar{2}}, \dots, x_{\bar{n}_{\text{out}}} \rangle. \end{aligned}$$

Suppose G_{out} has s_{out} conserved quantities denoted $H_1, \dots, H_{s_{\text{out}}}$ and suppose G_{in} has s_{in} conserved quantities denoted, $F_1, \dots, F_{s_{\text{in}}}$. We will assume the Hamiltonians are,

$$\begin{aligned} H_1(x_{\bar{1}}, \dots, x_{\bar{n}_{\text{out}}}) &= x_{\bar{1}} + \dots + x_{\bar{n}_{\text{out}}} \quad \text{and} \\ F_1(x_1, \dots, x_{n_{\text{in}}}) &= x_1 + \dots + x_{n_{\text{in}}}. \end{aligned}$$

Necessarily, G_{out} has at most one Casimir containing x_1 . For simplicity, denote this Casimir as C with corresponding eigenvector for \mathbf{A}_{out} , $\boldsymbol{\chi} = \langle \chi_1, \dots, \chi_{n_{\text{out}}} \rangle$. Our assumption that G_{out} admits Itoh-style conserved quantities implies that $\boldsymbol{\chi}$ is made up of ones and zeros with $\chi_1 = 1$. This function C is among the functions $H_1, \dots, H_{n_{\text{out}}}$ and there may be other Casimirs not containing x_1 .

Our assumption that G_{in} and G_{out} admit Itoh-style conserved quantities implies that we can write each of the conserved quantities of G_{out} and G_{in} as,

$$H_i(x_{\bar{1}}, \tilde{\mathbf{x}}_{\text{out}}) = \sum_{l \in \mathcal{U}_i} x_{\bar{1}} P_l(\tilde{\mathbf{x}}_{\text{out}}) + \sum_{l \in \mathcal{V}_i} Q_l(\tilde{\mathbf{x}}_{\text{out}}) \quad (11)$$

$$F_i(\mathbf{x}_{\text{in}}) = \sum_{l \in \mathcal{W}_i} A_l(\mathbf{x}_{\text{in}}), \quad (12)$$

where P_l , Q_l and A_l are monomials and \mathcal{U}_i , \mathcal{V}_i and \mathcal{W}_i are appropriately defined index sets over the terms of the conserved quantities H_i and F_i . See Eq. (10). Also, an example is given in Eq. (7) for the cycle graphs. In particular, the Casimir C will have form $C = x_1 P(\tilde{\mathbf{x}}_{\text{out}})$.

The following procedure can be used to construct the new conserved quantities for J :

- (i) Using the Casimir C of G_{out} containing the variable x_1 and the non-Hamiltonian conserved quantities of G_{in} define,

$$\Gamma_i(\mathbf{x}_{\text{in}}, \tilde{\mathbf{x}}_{\text{out}}) = F_i(\mathbf{x}_{\text{in}})^{\chi_1} P(\tilde{\mathbf{x}}_{\text{out}})^r, \quad (13)$$

for $i \in \{2, \dots, s_{\text{in}}\}$. Here r is the order of F_i as a polynomial. Note that we have replaced x_1 in C with $F_i(\mathbf{x}_{\text{in}})$. Recall by assumption $\chi_1 = 1$, but we leave it explicit for clarity in the proof. We show that when F_i is a Casimir of G_{in} , then Γ_i is a Casimir of J .

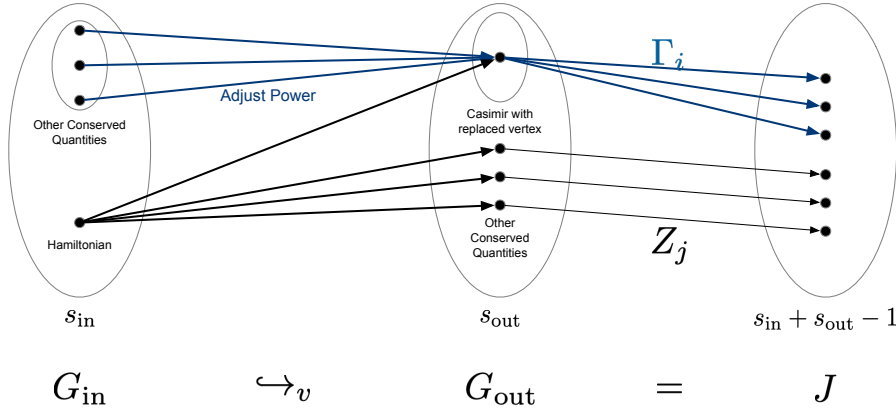


Figure 5. To construct conserved quantities for an embedding of two Bogoyavlenskij graphs, first replace all instances of the variable representing the embedding vertex in the Casimirs of the outer graph with the conserved quantities from the inner graph, correcting the power of the remaining terms appropriately. Then replace all instances of the variable representing the embedding vertex with the Hamiltonian of the inner graph in non-Casimir conserved quantities of the outer graph.

- (ii) Using the Hamiltonian $F_1(\mathbf{x}_{\text{in}})$ of G_{in} and every conserved quantity of G_{out} that contains x_1 define,

$$Z_i = \sum_{l \in \mathcal{U}_i} F_1(\mathbf{x}_{\text{in}}) P_l(\tilde{\mathbf{x}}_{\text{out}}) + \sum_{l \in \mathcal{V}_i} Q_l(\tilde{\mathbf{x}}_{\text{out}}). \quad (14)$$

That is, we replace x_1 in H_i with $F_1(\mathbf{x}_{\text{in}})$. Any other remaining conserved quantities that do not contain x_1 are carried forward to J , which can also be thought of as replacing x_1 with F_1 in a trivial way.

The procedure is illustrated in Fig. 5.

Claim 1. *The quantities defined in Eq. (13) are conserved.*

Proof. By assumption, there are vectors α_l so that,

$$\frac{dA_l}{dt} = A_l(\mathbf{x}_{\text{in}}) \alpha_l^T \mathbf{A}_{\text{in}} \mathbf{x}_{\text{in}},$$

with,

$$\frac{dF_i}{dt} = \sum_{l \in \mathcal{W}_i} A_l(\mathbf{x}_{\text{in}}) \alpha_l^T \mathbf{A}_{\text{in}} \mathbf{x}_{\text{in}} = 0. \quad (15)$$

Likewise, for the eigenvector vector $\chi = \langle \chi_1, \dots, \chi_{n_{\text{out}}} \rangle$, we have,

$$\frac{dC}{dt} = C \chi^T \mathbf{A}_{\text{out}} \mathbf{x}_{\text{out}} = 0.$$

The vectors α_l and χ_j are just the powers appearing in the monomials A_l and Casimir C_j . In particular, χ is an eigenvector of \mathbf{A}_{out} . To be explicit, let $\bar{\chi} = \langle \chi_2, \dots, \chi_{n_{\text{out}}} \rangle$. We

know from, Eq. (2), that,

$$\boldsymbol{\chi}^T \mathbf{A}_{\text{out}} = \begin{bmatrix} \chi_1 & \bar{\boldsymbol{\chi}}^T \end{bmatrix} \begin{bmatrix} 0 & \mathbf{r}^T \\ -\mathbf{r} & \tilde{\mathbf{A}}_{\text{out}} \end{bmatrix} = \begin{bmatrix} -\bar{\boldsymbol{\chi}}^T \mathbf{r} & \chi_1 \mathbf{r}^T + \bar{\boldsymbol{\chi}}^T \tilde{\mathbf{A}}_{\text{out}} \end{bmatrix} = \mathbf{0}.$$

Thus, we have the identities,

$$\bar{\boldsymbol{\chi}}^T \mathbf{r} = 0 \quad (16)$$

$$\chi_1 \mathbf{r}^T + \bar{\boldsymbol{\chi}}^T \tilde{\mathbf{A}}_{\text{out}} = \mathbf{0}, \quad (17)$$

which can be interpreted as a kind of flow balance equations. By construction, $\Gamma_i = F_i(\mathbf{x}_{\text{in}})P(\tilde{\mathbf{x}}_{\text{out}})$ is just a sum of monomials. To account for the embedding and to be notationally consistent, let $\tilde{\boldsymbol{\chi}}_j = \langle \chi_{\tilde{2}}, \dots, \chi_{\tilde{n}_{\text{out}}} \rangle$.

Consequently, there are vectors $\boldsymbol{\gamma}_l = \langle \chi_1 \boldsymbol{\alpha}_l, r \tilde{\boldsymbol{\chi}} \rangle$ so that,

$$\begin{aligned} \frac{d\Gamma_i}{dt} &= \sum_{l \in \mathcal{W}_i} A_l P^r \boldsymbol{\gamma}_l^T \mathbf{A} \mathbf{x} = \\ &\sum_{l \in \mathcal{W}_i} A_l P^r \left[(\chi_1 \boldsymbol{\alpha}_l^T \mathbf{A}_{\text{in}} - r \tilde{\boldsymbol{\chi}}^T \mathbf{R}) \mathbf{x}_{\text{in}} + (\chi_1 \boldsymbol{\alpha}_l^T \mathbf{R}^T + r \tilde{\boldsymbol{\chi}}^T \tilde{\mathbf{A}}_{\text{out}}) \tilde{\mathbf{x}}_{\text{out}} \right]. \end{aligned}$$

Recall, r is the order of F_i . From the structure of \mathbf{R} , see Eq. (4), we see that,

$$\boldsymbol{\alpha}_l^T \mathbf{R}^T = r \mathbf{r}^T. \quad (18)$$

Likewise, we have from Eq. (16) we see,

$$\tilde{\boldsymbol{\chi}}^T \mathbf{R} = \mathbf{0} \quad (19)$$

Therefore, from Eqs. (15) to (19) we have,

$$\begin{aligned} \frac{d\Gamma_i}{dt} &= P^r \sum_{l \in \mathcal{W}_i} A_l \boldsymbol{\alpha}_l^T \mathbf{A}_{\text{in}} \mathbf{x}_{\text{in}} - r P^r \sum_{l \in \mathcal{W}_i} A_l \tilde{\boldsymbol{\chi}}^T \mathbf{R} \mathbf{x}_{\text{in}} + \\ &P^r \sum_{l \in \mathcal{W}_i} r A_l (\chi_1 \mathbf{r}^T + \bar{\boldsymbol{\chi}}^T \tilde{\mathbf{A}}_{\text{out}}) \tilde{\mathbf{x}}_{\text{out}} = 0. \end{aligned}$$

□

From the proof of this claim, it's immediately clear that if F_i is a Casimir of G_{in} , then there is only one term in the sum and the resulting vector $\boldsymbol{\gamma}_i$ must be an eigenvector of \mathbf{A} with eigenvalue 0 and therefore Γ_i is a Casimir of the new system.

Claim 2. *The quantities defined in Eq. (14) are conserved.*

Proof. This follows from the use of the Hamiltonian $F_1(\mathbf{x}_{\text{in}})$ in Eq. (14) and the fact that $x_{\bar{1}}$ is being replaced by $x_1, \dots, x_{n_{\text{in}}}$ and Z_i is constructed from the conserved quantity in Eq. (11). That is, we are simply renaming $x_{\bar{1}}$ and this will not affect the time derivative of the quantity. □

Claim 3. *The constructed conserved quantities commute under the action of the quadratic bracket in Eq. (5).*

Proof. It suffices to consider two functions of form,

$$\Gamma_\alpha = F_\alpha(\mathbf{x}_{\text{in}})P_\alpha(\tilde{\mathbf{x}}_{\text{out}})^{r_\alpha} \quad \Gamma_\beta = F_\beta(\mathbf{x}_{\text{in}})P_\beta(\tilde{\mathbf{x}}_{\text{out}})^{r_\beta},$$

under the assumption that F_α and F_β commute under the bracket restricted to \mathbf{x}_{in} and $x_1^{r_\alpha} P_\alpha(\tilde{\mathbf{x}}_{\text{out}})^{r_\alpha}$ and $x_1^{r_\beta} P_\beta(\tilde{\mathbf{x}}_{\text{out}})^{r_\beta}$ commute under the bracket restricted to \mathbf{x}_{out} . Here r_α is the order of the polynomial F_α and r_β is the order of the polynomial F_β .

In what follows, we assume that $1 < \dots < n_{\text{in}} < \bar{2} < \dots < \bar{n}_{\text{out}}$. That is, the bar indicates an appropriate index shift as a result of the embedding. Consider the bracket,

$$\{\Gamma_\alpha, \Gamma_\beta\}_{\mathbf{A}} = \sum_{i < j} A_{ij} x_i x_j \underbrace{\left(\frac{\partial F_\alpha P_\alpha^{r_\alpha}}{\partial x_i} \frac{\partial F_\beta P_\beta^{r_\beta}}{\partial x_j} - \frac{\partial F_\alpha P_\alpha^{r_\alpha}}{\partial x_j} \frac{\partial F_\beta P_\beta^{r_\beta}}{\partial x_i} \right)}_{\Xi}$$

Denote the term under the sum by Ξ . When $i < j \leq n_{\text{in}}$, then Ξ simplifies to,

$$P_\alpha^{r_\alpha} P_\beta^{r_\beta} A_{ij} x_i x_j \left(\frac{\partial F_\alpha}{\partial x_i} \frac{\partial F_\beta}{\partial x_j} - \frac{\partial F_\alpha}{\partial x_j} \frac{\partial F_\beta}{\partial x_i} \right),$$

which vanishes under the sum because F_α and F_β commute.

Now consider the remaining elements of the sum with $j \geq \bar{2}$. The assumption that the graphs admit Itoh-style conserved quantities is now critical. Assume Ξ does not evaluate to zero. If $i \geq \bar{2}$, then both derivatives affect the terms $P_\alpha^{r_\alpha}$ and $P_\beta^{r_\beta}$. We have,

$$\begin{aligned} \Xi &= A_{ij} x_i x_j \left(\frac{\partial F_\alpha P_\alpha^{r_\alpha}}{\partial x_i} \frac{\partial F_\beta P_\beta^{r_\beta}}{\partial x_j} - \frac{\partial F_\alpha P_\alpha^{r_\alpha}}{\partial x_j} \frac{\partial F_\beta P_\beta^{r_\beta}}{\partial x_i} \right) = \\ &A_{ij} (r_\alpha r_\beta F_\alpha F_\beta P_\alpha^{r_\alpha} P_\beta^{r_\beta} - r_\alpha r_\beta F_\alpha F_\beta P_\alpha^{r_\alpha} P_\beta^{r_\beta}) = 0, \end{aligned}$$

because the $x_i x_j$ multiplier effectively removes the differentiation in the functions $P_\alpha^{r_\alpha}$ and $P_\beta^{r_\beta}$.

This leaves the case when $i \leq n_{\text{in}}$ and $j \geq \bar{2}$. Here we have,

$$\Xi = \underbrace{r_\beta A_{ij} F_\alpha F_\beta P_\alpha^{r_\alpha} P_\beta^{r_\beta}}_{T_1} - \underbrace{r_\alpha A_{ij} F_\alpha F_\beta P_\alpha^{r_\alpha} P_\beta^{r_\beta}}_{T_2}$$

However, because the order of F_α is r_α , the term T_1 will occur r_α times in the sum, while the term T_2 will occur r_β times in the sum because F_β has order r_β . Thus, when summing over all i indices occurring in F_α and F_β , the sum will produce,

$$r_\alpha r_\beta A_{ij} F_\alpha F_\beta P_\alpha^{r_\alpha} P_\beta^{r_\beta} - r_\beta r_\alpha A_{ij} F_\alpha F_\beta P_\alpha^{r_\alpha} P_\beta^{r_\beta} = 0.$$

It follows immediately that any pair of constructed conserved quantities commute under the quadratic bracket. \square

It now suffices to show that there are a sufficient number of conserved quantities to ensure that the resulting dynamics generated by the graph J are integrable. The fact that they are algebraically independent is immediately clear from the construction. Let c_{in} and c_{out} be the total number of Casimirs in G_{in} and G_{out} respectively. By construction, J has at least $c_{\text{in}} + c_{\text{out}} - 1$ Casimirs consisting of the c_{in} Γ_i that were constructed and the remaining $c_{\text{out}} - 1$ Casimirs that do not contain x_1 . However, it follows from the structure of \mathbf{A} that these are the only possible Casimirs, as any other Casimirs would have the form $F_i(\mathbf{x}_{\text{in}})Q(\mathbf{x}_{\text{out}})$, where Q is yet another Casimir of G_{out} containing x_1 . Consequently, we have:

$$\begin{aligned} \text{Rank}(\mathbf{A}) &= (n_{\text{in}} + n_{\text{out}} - 1) - (c_{\text{in}} + c_{\text{out}} - 1) = (n_{\text{in}} - c_{\text{in}}) + (n_{\text{out}} - c_{\text{out}}) = \\ & \qquad \qquad \qquad \text{Rank}(\mathbf{A}_{\text{in}}) + \text{Rank}(\mathbf{A}_{\text{out}}). \end{aligned}$$

As illustrated in Fig. 5, we have constructed $s_{\text{in}} + s_{\text{out}} - 1$ conserved quantities. From Definition 2.8 and our assumption on the integrability of G_{in} and G_{out} we know that,

$$\begin{aligned} s_{\text{in}} + \frac{1}{2}\text{Rank}(\mathbf{A}_{\text{in}}) &= n_{\text{in}} \\ s_{\text{out}} + \frac{1}{2}\text{Rank}(\mathbf{A}_{\text{out}}) &= n_{\text{out}}. \end{aligned}$$

Adding these quantities together and subtracting 1 yields,

$$s_{\text{in}} + s_{\text{out}} - 1 + \frac{1}{2}\text{Rank}(\mathbf{A}) = n_{\text{in}} + n_{\text{out}} - 1.$$

It follows at once that the dynamics generated by J are integrable. This completes the proof. \square

The simplest example of this process is the embedding of a directed three cycle into another directed three cycle, which is used as an ecological model by Allesina et al. [18] and shown to be integrable by Paik and Griffin [11] in their discussion on the integrability of tournament embeddings, which is generalised by Theorem 4.2. Instead, we illustrate the more complex case by embedding a directed three-cycle into a directed four-cycle, as illustrated in Fig. 1. The conserved quantities for G_{in} are,

$$F_1 = x_1 + x_2 + x_3 \quad \text{and} \quad F_2 = x_1x_2x_3.$$

The conserved quantities for G_{out} are,

$$H_1 = x_1 + x_2 + x_3 + x_4, \quad H_2 = x_1x_3, \quad \text{and} \quad H_3 = x_2x_4.$$

Notice, G_{out} has two Casimirs, H_2 and H_3 , only one of which contains x_1 . We have,

$$\Gamma_1 = \underbrace{(x_1x_2x_3)}_{F_2} \underbrace{x_3^3}_{P^3},$$

and

$$Z_1 = x_1 + x_2 + x_3 + x_{\bar{2}} + x_{\bar{3}} + x_{\bar{4}} \quad (20)$$

$$Z_2 = (x_1 + x_2 + x_3)x_{\bar{3}} \quad (21)$$

$$Z_3 = x_2x_4 \quad (22)$$

Direct inspection shows that these are conserved quantities under the replicator dynamics generated by the graph shown in Fig. 1 and that they are algebraically independent and commute under the action of the bracket.

Before concluding this section, it is worth noting that the matrix of the embedded graph need not have only $0, \pm 1$ entries. The matrix, corresponding to \mathbf{A}_{in} can be multiplied by any constant, effectively speeding up the dynamics in this subpopulation of variables, without changing the integrability of the system. This allows us to extend our results to a broader class of interaction matrices and potential make formal statements about the integrability of dynamics that exhibit multiple, hierarchical time scales. We omit a formal analysis of this observation and leave it for future work.

5. Multiple Simultaneous Embeddings

Paik and Griffin note in [11] that this embedding procedure can be generalised to multiple simultaneous embeddings to produce integrable (tournament) graphs. We now assume that multiple graphs with Itoh-style conserved quantities are being embedded into a single graph also with Itoh-style conserved quantities. For this, we use the notation,

$$J = (G_{\text{in}}^1, \dots, G_{\text{in}}^m) \hookrightarrow_{(v_1, \dots, v_m)} G_{\text{out}}. \quad (23)$$

For simplicity, we now refer to the conserved quantities of graph G_{in}^j (with $j \in \{1, \dots, m\}$) as F_i^j with $i \in \{1, \dots, s_{\text{in}}^j\}$ and the conserved quantities of G_{out} by H_i for $i \in \{1, \dots, s_{\text{out}}\}$. Without loss of generality, we assume that the vertices into which we are embedding are ordered so that $v_i = i$ for $i \in \{1, \dots, m\}$. By assumption, the conserved quantities of G_{out} can be written as,

$$H_i = \sum_{l \in \mathcal{U}_i} B_l(x_1, \dots, x_{n_{\text{out}}}),$$

where B_l is a monomial (product) and \mathcal{U}_i is an appropriate index set (as before). Also, any Casimir C_i of G_{out} containing x_{i_1}, \dots, x_{i_k} for $1 \leq i_1 < \dots < i_k \leq m$ can be written,

$$C_i(\mathbf{x}_{\text{out}}) = x_{i_1} \cdots x_{i_k} P_i^{i_1, \dots, i_k}(\tilde{\mathbf{x}}_{\text{out}}),$$

where, the definition of $\tilde{\mathbf{x}}_{\text{out}}$ is modified appropriately and $P_i^{i_1, \dots, i_k}$ is an appropriate monomial.

To build the conserved quantities of $J = (G_{\text{in}}^1, \dots, G_{\text{in}}^m) \hookrightarrow_{(v_1, \dots, v_m)} G_{\text{out}}$, we use the following procedure, which generalises the one illustrated in Fig. 5.

- (i) Suppose $C_i(\mathbf{x}_{\text{out}}) = x_{i_1} \cdots x_{i_k} P(\tilde{\mathbf{x}}_{\text{out}})$ is a Casimir of G_{out} containing x_{i_1}, \dots, x_{i_k} , where i_1, \dots, i_k are a subset of the indices into which $(G_{\text{in}}^1, \dots, G_{\text{in}}^m)$ are embedded. Let $H_{j_1}^{i_1}, \dots, H_{j_k}^{i_k}$ be conserved quantities of G^{i_1}, \dots, G^{i_k} with orders r_{i_1}, \dots, r_{i_k} . Let $r = \max\{r_{i_1}, \dots, r_{i_k}\}$. Then,

$$\Gamma_{i, j_1, \dots, j_k}^{i_1, \dots, i_k} = (H_{j_1}^{i_1})^{r/r_{i_1}} \cdots (H_{j_k}^{i_k})^{r/r_{i_k}} (P_i^{i_1, \dots, i_k})^r,$$

is a conserved quantity and when $H_{j_1}^{i_1}, \dots, H_{j_k}^{i_k}$ are all Casimirs of $G_{\text{in}}^{i_1}, \dots, G_{\text{in}}^{i_k}$, then the conserved quantity is a Casimir of J .

- (ii) Suppose $H_i(\mathbf{x}_{\text{out}})$ is a non-Casimir conserved quantity of G_{out} containing x_{i_1}, \dots, x_{i_k} , where i_1, \dots, i_k are a subset of the indices into which $(G_{\text{in}}^1, \dots, G_{\text{in}}^m)$ are embedded. Let $H_1^{i_1}, \dots, H_1^{i_k}$ be the Hamiltonians of the input graphs $G_{\text{in}}^{i_1}, \dots, G_{\text{in}}^{i_k}$. Then,

$$Z_{i, i_1, \dots, i_k} = \sum_{l \in \mathcal{U}_i} (H_1^{i_1}, \dots, H_1^{i_k}, \tilde{\mathbf{x}}_{\text{out}}),$$

is also a conserved quantity.

This can be summarised as follows: First, replace the x_1, \dots, x_m in the Casimir(s) of G_{out} with any combination of conserved quantities from the corresponding input graphs, being sure that each term in the resulting product is of the same polynomial order by raising the terms to an appropriate power. Then replace x_1, \dots, x_m in any other non-Casimir conserved quantities of G_{out} with the Hamiltonians of $G_{\text{in}}^1, \dots, G_{\text{in}}^m$. This will produce the conserved quantities of J .

To illustrate this procedure, consider the embedding of two directed five-cycles into a third skip graph with six vertices, as shown in Fig. 6. We have labelled the vertices

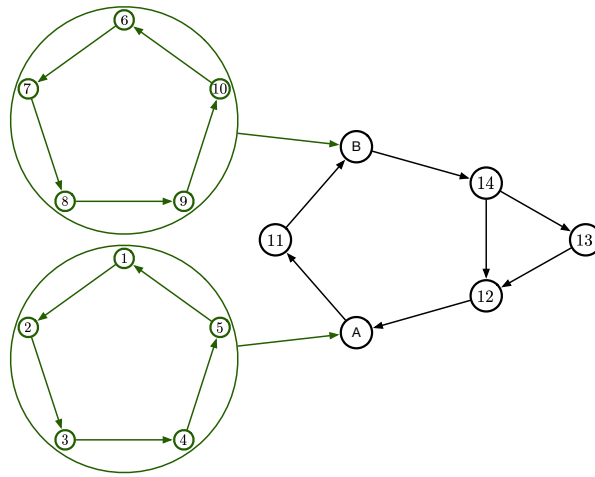


Figure 6. When we embed two directed five-cycles into a skip-graph with six vertices, we require eight algebraically independent conserved quantities, which can be constructed using the conserved quantities of the constituent graphs.

for simplicity in constructing the conserved quantities. The conserved quantities for one

of the five cycles are,

$$\begin{aligned} F_1 &= x_1 + x_2 + x_3 + x_4 + x_5 \\ F_2 &= x_1x_3 + x_5x_3 + x_1x_4 + x_2x_4 + x_2x_5 \\ F_3 &= x_1x_2x_3x_4x_5. \end{aligned}$$

The conserved quantities for the skip-graph, in terms of their labelled vertices, are,

$$\begin{aligned} H_1 &= x_A + x_B + x_{11} + x_{12} + x_{13} + x_{14} \\ H_2 &= x_Ax_B + x_Ax_{13} + x_Ax_{14} + x_Bx_{12} + x_Bx_{13} + x_{11}x_{12} + x_{11}x_{13} + x_{11}x_{14} \\ H_3 &= x_Ax_Bx_{13} \\ H_4 &= x_Ax_Bx_{11}x_{12}x_{14} \end{aligned}$$

We now organise the constructed conserved quantities into groups depending on which classes of inner-graph conserved quantities are substituted into the outer-graph conserved quantities.

Group 1: Casimirs into Casimir

$$\begin{aligned} &(x_1x_2x_3x_4x_5)(x_6x_7x_8x_9x_{10})x_{11}^5x_{12}^5x_{14}^5 \\ &(x_1x_2x_3x_4x_5)(x_6x_7x_8x_9x_{10})x_{13}^5 \end{aligned}$$

Group 2: Mixed Casimir and Second Order Conserved Quantities in Casimir

$$\begin{aligned} &x_1x_2x_3x_4x_5(x_6x_8 + x_{10}x_8 + x_6x_9 + x_7x_9 + x_7x_{10})^{5/2}x_{11}^5x_{12}^5x_{14}^5 \\ &x_1x_2x_3x_4x_5(x_6x_8 + x_{10}x_8 + x_6x_9 + x_7x_9 + x_7x_{10})^{5/2}x_{13}^5 \\ &(x_1x_3 + x_5x_3 + x_1x_4 + x_2x_4 + x_2x_5)^{5/2}x_6x_7x_8x_9x_{10}x_{11}^5x_{12}^5x_{14}^5 \\ &(x_1x_3 + x_5x_3 + x_1x_4 + x_2x_4 + x_2x_5)^{5/2}x_6x_7x_8x_9x_{10}x_{13}^5 \end{aligned}$$

Group 3: Second Order Conserved Quantities in Casimir

$$\begin{aligned} &(x_1x_3 + x_5x_3 + x_1x_4 + x_2x_4 + x_2x_5)(x_6x_8 + x_{10}x_8 + x_6x_9 + x_7x_9 + x_7x_{10})x_{11}^2x_{12}^2x_{14}^2 \\ &(x_1x_3 + x_5x_3 + x_1x_4 + x_2x_4 + x_2x_5)(x_6x_8 + x_{10}x_8 + x_6x_9 + x_7x_9 + x_7x_{10})x_{13}^2 \end{aligned}$$

Group 4: Mixed Hamiltonians and Second Order Conserved Quantities in Casimir

$$\begin{aligned} &(x_1 + x_2 + x_3 + x_4 + x_5)^2(x_6x_8 + x_{10}x_8 + x_6x_9 + x_7x_9 + x_7x_{10})x_{11}^2x_{12}^2x_{14}^2 \\ &(x_1 + x_2 + x_3 + x_4 + x_5)^2(x_6x_8 + x_{10}x_8 + x_6x_9 + x_7x_9 + x_7x_{10})x_{13}^2 \\ &(x_1x_3 + x_5x_3 + x_1x_4 + x_2x_4 + x_2x_5)(x_6 + x_7 + x_8 + x_9 + x_{10})^2x_{11}^2x_{12}^2x_{14}^2 \\ &(x_1x_3 + x_5x_3 + x_1x_4 + x_2x_4 + x_2x_5)(x_6 + x_7 + x_8 + x_9 + x_{10})^2x_{13}^2 \end{aligned}$$

Group 5: Hamiltonians in Casimir

$$\begin{aligned} &(x_1 + x_2 + x_3 + x_4 + x_5)(x_6 + x_7 + x_8 + x_9 + x_{10})x_{11}x_{12}x_{14} \\ &(x_1 + x_2 + x_3 + x_4 + x_5)(x_6 + x_7 + x_8 + x_9 + x_{10})x_{13} \end{aligned}$$

Group 6: Hamiltonians in Second Order Conserved Quantity

computations were performed in Mathematica, version 14. Except for one figure, all graphs shown in this section were automatically laid out with Mathematica as well. Of those 21,419 graphs, we find that 57 are integrable. We suspect that 184 graphs produce chaotic behaviour, as a result of numerical evaluation. The remaining 21,178 graphs asymptotically decay to a lower-order system and do not have an interior fixed point in a higher-order unit simplex. This is summarised in Table 1

Vertex Count	Integrable	Suspected Chaotic	No Interior Fixed Point	Total
3	1	0	1	2
4	3	0	31	34
5	11	4	520	535
6	42	180	20,626	20,848
Totals	57	184	21,178	21,419

Table 1. Breakdown by vertex size of all graphs that are integrable

To derive these statistics, we used Brendan McKay’s database of graphs [34]. We first identified those graphs that were strongly connected; i.e., those graphs for which there is a directed path between any pair of vertices [35]. The dynamics of these graphs necessarily asymptotically decay to the dynamics of a lower-order system, as shown by Paik and Griffin [11]. This reduced the number of potentially integrable graphs down to 4,313.

To sort through these remaining graphs, we first found every graph that contained a sufficient number of Casimirs to be integrable. We then numerically identified the remaining graphs with an interior fixed point. It is possible, but not computationally efficient, to use Mathematica’s symbolic solver to identify these graphs. Instead, we numerically integrated the system of differential equations generated from each graph to obtain numerical flows $x_i(t)$, where i ranged over the number of vertices in the graph in question, using an initial condition $\mathbf{x} \in \text{int}(\Delta_{n-1})$ for appropriate n . We then numerically computed,

$$\bar{x}_i = \frac{1}{T_f - T_0} \int_{T_0}^{T_f} x_i(t) dt,$$

where $T_0 \gg 0$. Since the initial condition is in the interior of an appropriate unit simplex, we know that $\bar{x}_i > 0$ for all i if the dynamics admit an interior fixed point. If there is some i for which $\bar{x}_i < \tau$, where $\tau \ll 1$ is a threshold, we then the dynamics admit no interior fixed point, and they collapse to the boundary of Δ_{n-1} . In that case, the trajectories asymptotically approach the orbits of a lower-dimensional replicator equation. For our numerical experiments, we used $\tau = 10^{-6}$ and via Mathematica’s `Chop` function and we set $T_0 = 250$.

Finally, we used the Wolf Algorithm [36, 37] on each remaining graph to find numerical evidence of chaotic behaviour. Many of the graphs exhibit weak chaos with very small (but positive) Lyapunov exponents. Consequently, we ran the Wolf algorithm over several initial conditions for each graph to identify possible signs of

chaotic behaviour in the dynamics. If a graph was not ruled out using the Wolf algorithm, we proceeded under the assumption that it was integrable and identified its conserved quantities. In this way, all 21,419 were categorised (see Table 1).

While executing the Wolf Algorithm, we found that several 5 vertex graphs exhibited signs of numerical chaos, suggesting that these are the smallest possible graphs to produce chaotic dynamics. One of the simplest of these graphs is shown in Fig. 7 and appears to be an example of a coupled oscillator in the replicator dynamics, as it is composed of two directed three cycles joined at a single vertex. While we have not

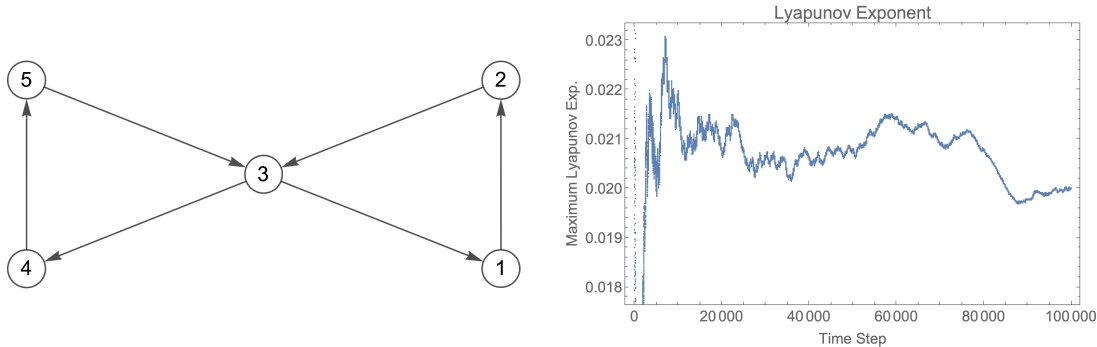


Figure 7. (Left) A simple graph that produces chaotic dynamics appears to be a coupled oscillator. (Right) Output of the Wolf Algorithm indicating that the system has positive Lyapunov exponent.

formally proved that this graph admits dynamics with positive Lyapunov exponent, its small size may make it amenable to such an analysis in future work.

In our investigation, we have found that, with limited exceptions, integrable graphs up to 6 vertices are characterised by a modification to a directed cycle (i.e., an element of the Volterra lattice). We note that this modification need not preserve symmetry, as shown by the skip-vertex graphs. Based on work presented in this paper as well as the previous work done by Bogoyavlenskij [8] and Evrpidou et al.[10], we can categorise all but three six vertex graphs into four families: Bogoyavlenskij graphs (denoted $B(n, k)$), Skip-vertex graphs, Cloned graphs and Embedding graphs. The remaining graphs are considered Holdout graphs. Raw counts of each family are shown in Table 2. We provide

Family	Vertex size				Total
	3	4	5	6	
$B(n, k)$	1	1	2	2	6
Skip-Vertex	0	1	0	3	4
Cloned	0	1	7	24	32
Embedding	0	0	1	11	12
Holdout	0	0	0	3	3

Table 2. Breakdown of Integrability by Family and Vertex Size

illustrative examples from each family below.

6.1. Bogoyavlenskij Family

The Bogoyavlenskij family consists of all graphs $B(n, k)$, including the tournament graphs with an odd number of vertices. Technically, tournaments with n even and $k = \frac{n}{2}$ are not Bogoyavlenskij graphs and are not integrable, as their dynamics asymptotically converge to a lower order replicator dynamic. Tournaments are considered separately by Bogoyavlenskij [24] and by Itoh [6], who provides Itoh-style conserved quantities. In [6], Itoh-style conserved quantities for all graphs in the Bogoyavlenskij family are provided. The Bogoyavlenskij family is characterised by their high degree of symmetry, as shown in Fig. 8. Notice the conserved quantities of these graphs are formed from combinations of cycles and non-cycles (non-edges).

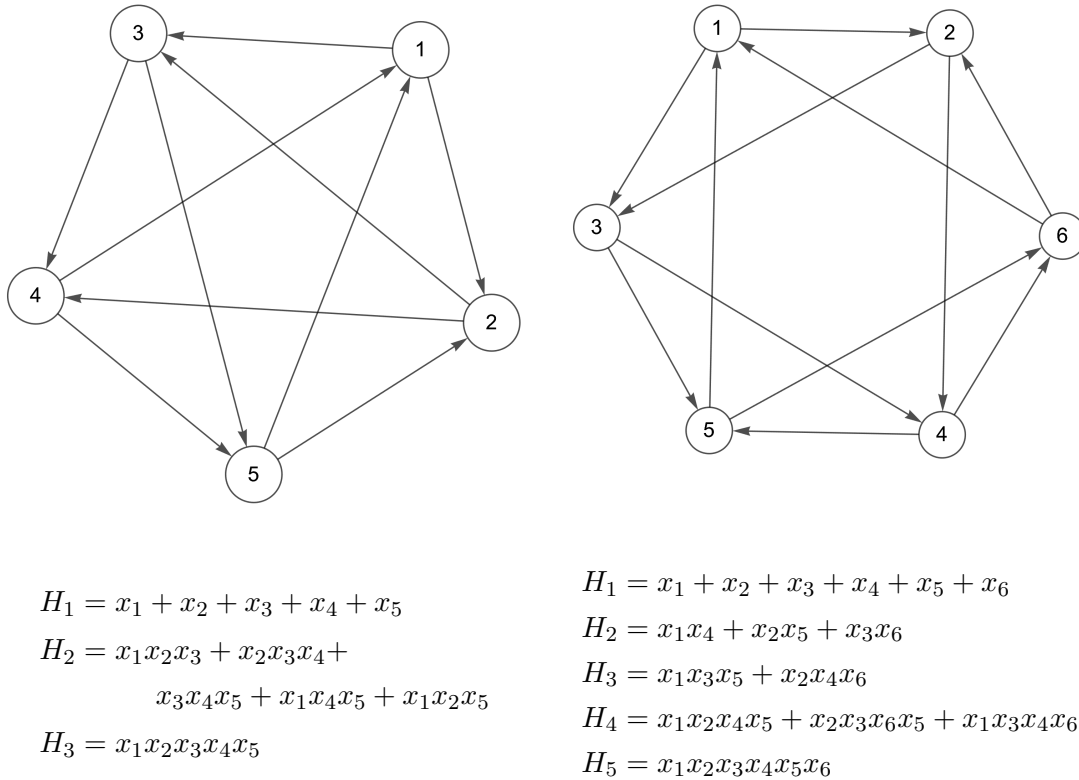
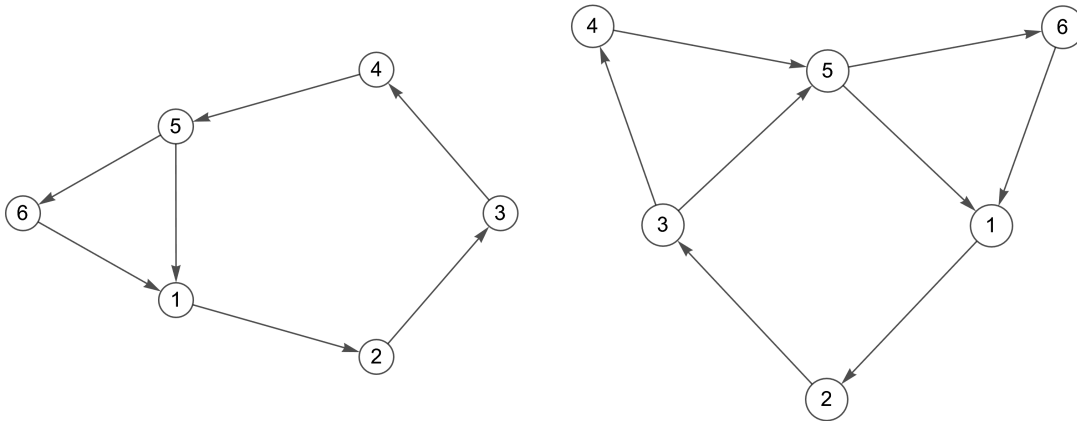


Figure 8. (Left) Balanced tournament graph with five vertices (species). (Right) Bogoyavlenskij graph with the maximum number of edges on six vertices. The conserved quantities are shown below their respective graphs.

6.2. Skip-Vertex Family

We showed that all members of the skip-vertex family are integrable in Theorem 3.5 and constructed their Itoh-style conserved quantities. There are 4 skip-vertex graphs with at most 6 vertices: one with 4 vertices, and three with 6 vertices. Two examples are shown in Fig. 9



$$H_1 = x_1 + x_2 + x_3 + x_4 + x_5 + x_6$$

$$H_2 = x_1x_3 + x_5x_3 + x_6x_3 + x_1x_4 + x_2x_4 + x_2x_5 + x_2x_6 + x_4x_6$$

$$H_3 = x_2x_4x_6$$

$$H_4 = x_1x_2x_3x_4x_5$$

$$H_1 = x_1 + x_2 + x_3 + x_4 + x_5 + x_6$$

$$H_2 = x_1x_3 + x_6x_3 + x_1x_4 + x_2x_4 + x_2x_5 + x_2x_6 + x_4x_6$$

$$H_3 = x_2x_4x_6$$

$$H_4 = x_1x_2x_3x_5$$

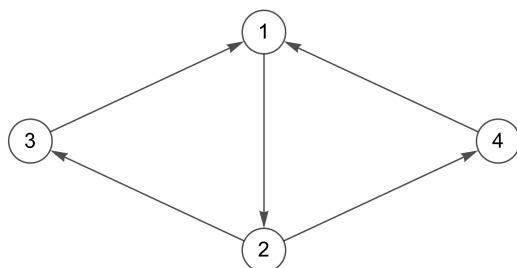
Figure 9. (Left) A skip-graph with one skipped vertex. (Right) A skip-graph with two skipped vertices. Note, both skipped vertices have the same parity.

6.3. Cloned Family

Recall that a graph with a cloned vertex has (at least) two vertices that share the same neighbourhood. The graph shown in Fig. 10 is the simplest possible example of a graph that is integrable as a result of cloning. Notice that Vertex 4 is a clone of Vertex 3. Removing Vertex 4, the operation referred to as decloning [10], reduces the graph to the directed three cycle, which is integrable. It follows from Theorem 2.11 that the graph shown in Fig. 10 is integrable. Evripidou et al. provide a mechanism for constructing conserved quantities using Lax pairs [10]. There are 32 graphs that are determined to be integrable through decloning. Interestingly, this is the largest subfamily of integrable graphs with six or fewer vertices. Notice this graph admits Itoh-style conserved quantities.

6.4. Embedding Family

There are 12 integrable graphs that are purely derived from embeddings: one graph with five vertices, and eleven with six vertices. We illustrate a directed four-cycle embedded into a directed three-cycle in Fig. 11, for comparison to the example from Fig. 1. Interestingly, there is overlap between the embedding family and the cloned family, as illustrated below. In our taxonomy, we count graphs in both the cloned and embedding families as embeddings first. We provide an example using the directed three-cycle embedded in the directed three-cycle, which was shown to be integrable by

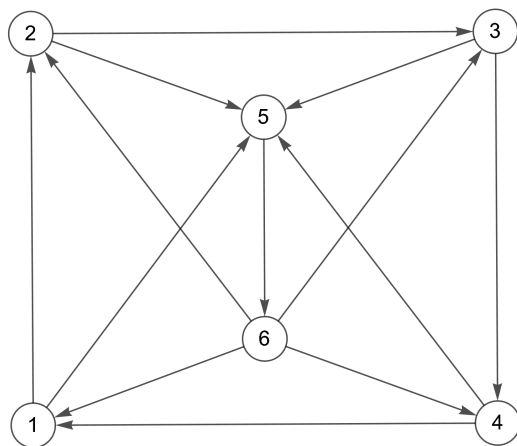


$$H_1 = x_1 + x_2 + x_3 + x_4$$

$$H_2 = x_1x_2x_3$$

$$H_3 = x_1x_2x_4$$

Figure 10. The simplest example of cloning to produce an integrable graph. Vertex 3 has the same neighbourhood as Vertex 4. Decloning produces the integrable directed three-cycle.



$$H_1 = x_1 + x_2 + x_3 + x_4 + x_5 + x_6$$

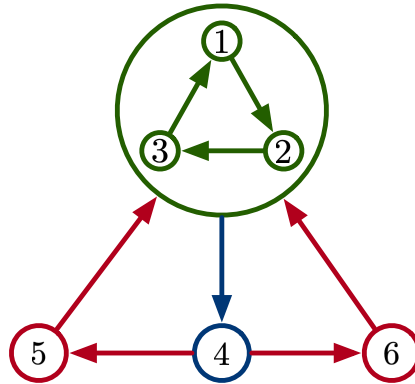
$$H_2 = (x_1 + x_2 + x_3 + x_4)x_5x_6$$

$$H_3 = x_1x_3x_5^2x_6^2$$

$$H_4 = x_2x_4x_5^2x_6^2$$

Figure 11. The directed four-cycle embedded into a directed three-cycle

Paik and Griffin [11] and was used by Allesina and Levine to model simple ecological systems [18]. Therefore, we refer to this graph as the AL graph. To construct the graph shown in Fig. 12, one can either clone Vertex 5 to create Vertex 6 from the AL graph (shown in red) or embed a directed three-cycle into Vertex 1 of the graph shown in Fig. 10. Notice this also nicely illustrates Theorem 4.2 in which we have a graph in the



$$H_1 = x_1 + x_2 + x_3 + x_4 + x_5 + x_6$$

$$H_2 = (x_1 + x_2 + x_3) x_4 (x_5 + x_6)$$

$$H_3 = x_1 x_2 x_3 x_4^3 x_5^3$$

$$H_4 = x_1 x_2 x_3 x_4^3 x_6^3$$

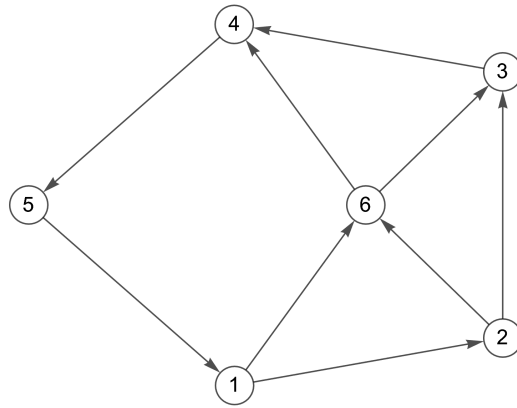
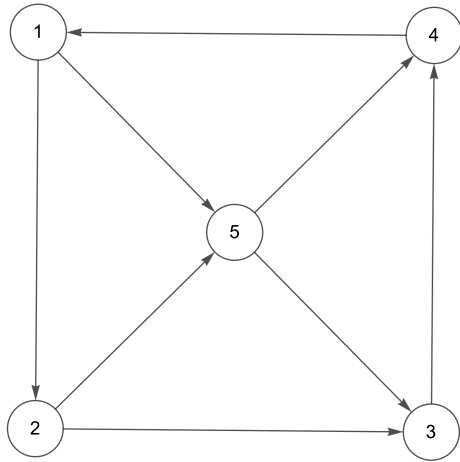
Figure 12. Example of a graph that is both an embedding and a cloning. This graph is a cloned version of the AL graph, with Vertices 5 and 6 cloned. It's also an embedding of the 3 cycle into Vertex 1 of the graph shown in Fig. 10.

Bogoyavlenskij family embedded into a graph in a graph that has Itoh-style conserved quantities but is not in the Bogoyavlenskij family.

6.5. Holdout Graphs

There are three integrable graphs that do not fall into any of these families. Of those three, two appear similar. They both are cycles (a four cycle and a five cycle, respectively) with an extra vertex with equal in and out degrees of two. The graphs and their corresponding conserved quantities are shown in Fig. 13. Notice these all have Itoh-style conserved quantities made of non-edges and cycles, as expected.

Further analysis suggests these graphs are part of a large family containing $n + 1$ vertices with two in-edges leading from Vertices i and $i + 1$ to Vertex $n + 1$ and two out-edges leading to Vertex $n + 1$ to Vertices $i + 2$ and $i + 3$. The next two graphs in this family are shown in Fig. 14. These graphs are integrable, having a sufficient number of commuting (Itoh-style) conserved quantities that commute. (See the SI for details.) It



$$\begin{aligned}
 H_1 &= x_1 + x_2 + x_3 + x_4 + x_5 \\
 H_2 &= x_1x_3 + x_2x_4 \\
 H_3 &= x_1x_4x_5 \\
 H_4 &= x_1x_2x_3x_4
 \end{aligned}$$

$$\begin{aligned}
 H_1 &= x_1 + x_2 + x_3 + x_4 + x_5 + x_6 \\
 H_2 &= x_1x_3 + x_1x_4 + x_2x_4 + \\
 &\quad x_2x_5 + x_3x_5 + x_5x_6 \\
 H_3 &= x_1x_4x_5x_6 \\
 H_4 &= x_1x_2x_3x_4x_5
 \end{aligned}$$

Figure 13. 2 Holdout graphs that appear to be related

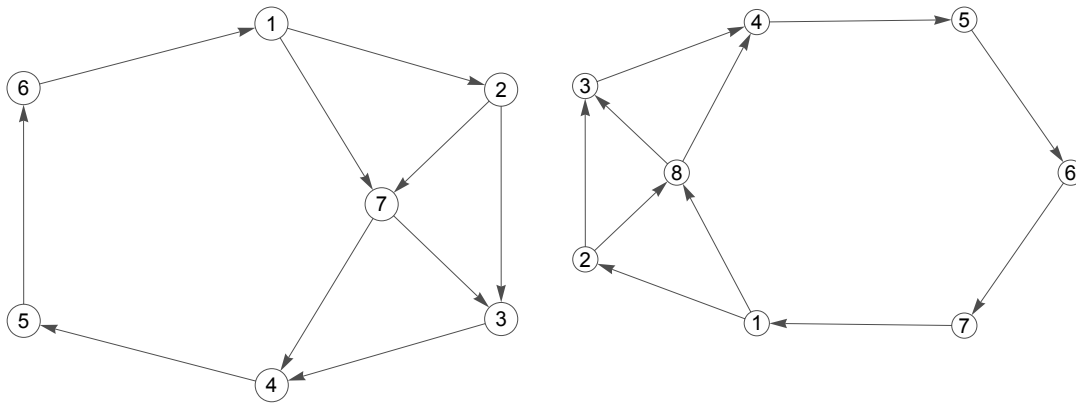
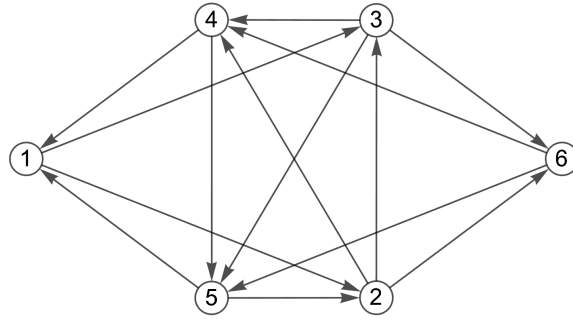


Figure 14. The next two elements of a “two-spoke” family are integrable, suggesting a new infinite family.

is left as future work whether these graphs are part of an even larger family related to wheel graphs, or if this characterisation is complete. We leave this analysis for future research. It is worth noting that these graphs also can be described as modifications of directed cycles.

One final integrable graph with six vertices stands alone. It can be described as a balanced tournament with an extra vertex. The balanced tournament is composed of Vertices 1-5. This is not the archetypal balanced tournament considered by Paik



$$H_1 = x_1 + x_2 + x_3 + x_4 + x_5 + x_6$$

$$H_2 = x_1x_2x_4 + x_1x_3x_4 + x_1x_3x_5 + x_2x_3x_5 + x_2x_4x_5 + x_2x_5x_6$$

$$H_3 = x_1x_6$$

$$H_4 = x_1x_2x_3x_4x_5$$

Figure 15. An unclassified hold-out graph exhibiting a form of chiral symmetry.

and Griffin [11] or that emerges from the Bogoyavlenskij construction[‡]. Instead, it is isomorphic to this archetype. Vertex 6 has the opposite neighbourhood to Vertex 1. The graph and its conserved quantities are shown in Fig. 15. This graph suggests the potential for another operation, ‘anti-cloning’, in which a vertex is introduced with a mirror image neighbourhood, imposing a kind of chiral symmetry into the graph. However, when this operation is performed on the 5-cycle, the resulting graph is in the family of graphs suspected of chaotic behaviour by numerical analysis. Thus, this final graph indicates that, while we have been able to categorise the vast majority of the integrable graphs, there are still missing pieces to this puzzle to consider in future work.

7. Discussion and Future Directions

In this paper, we generalised the concept of embeddings first introduced by Paik and Griffin [11]. While Paik and Griffin showed that embeddings of tournaments were integrable, we extended this concept to show that any (set of) integrable graphs with Itoh-style conserved quantities can be embedded into another integrable graph with Itoh-style conserved quantities to produce an integrable graph. We also introduced a new family of integrable graphs (the skip-graph family) and used these graphs along with our results on graph embeddings and the prior work by Evripidou et al. [10] to completely characterise the behaviour of the dynamics generated by all 21,419 oriented directed graphs with six or fewer vertices. In particular, we found 57 distinct integrable graphs, of which 54 fit into a taxonomy of four categories. Three hold-out graphs suggest

[‡] The archetypal balanced tournament on five vertices describes rock-paper-scissors-Spock-Lizard, in that order.

the existence of both new integrable families as well as graph operations that preserve integrability.

In addition to the integrable dynamics we have discussed, our analysis of graph structures and their resulting dynamics shows numerical evidence for Hamiltonian chaos (including weak chaos). In some cases (e.g., the graph shown in Fig. 7), the dynamics are simple enough that they may admit a formal proof for the existence of positive Lyapunov exponents. Of note, this chaotic behaviour is a function of the graph structure itself, a property also observed by Griffin et al. in networked replicator dynamics [38]. For some graphs, simple addition (or subtraction) of an edge will dramatically alter the underlying dynamics. For example, the graph shown in Fig. 16 produces chaotic behaviour, but removing the edge from Vertex 2 to Vertex 5 recovers the directed five cycle, an integrable graph. This suggests the dynamics arising from graphs may be

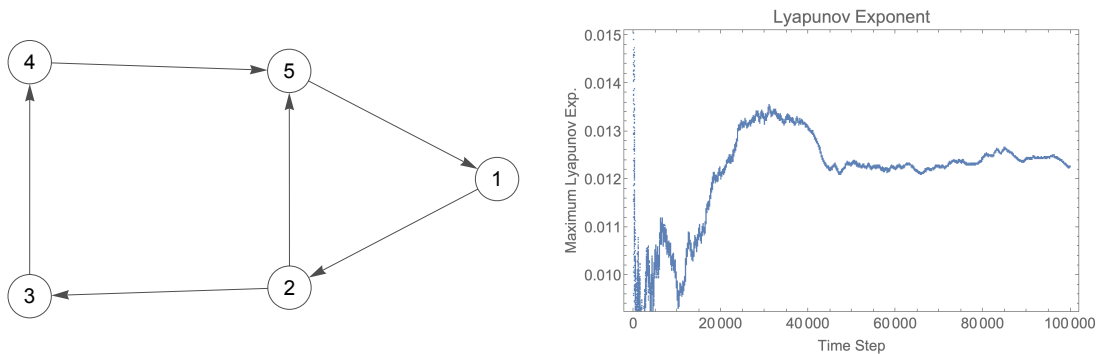


Figure 16. A graph that produces chaotic behaviour, but that will produce integrable (quasi-periodic) behaviour if a single edge is removed.

ideal toy models for experimenting with the effects of the emergence and destruction of feedback loops in complex systems. Such feedback loops are known to occur in both biological and environmental dynamics, making the models and results presented in this paper potentially relevant in understanding complex natural systems.

In summary, this work represents a continuation of work begun by Moser, Kac and van Moerbeke on the Volterra lattice and extended by Itoh, Bogoyavlenskij and Evripidou, Kassotakis and Vanhaecke. However, when taken as a whole, it suggests a program of research far more extensive in scope. There is a structure to the graphs that generate integrable replicator (Lotka-Volterra) dynamics, with families of “seed graphs” being used in cloning or embedding operations to generate sets of integrable graphs. It is unclear how many of these seed graph families there are, and whether they are all related in some way to the directed cycle, as we suspect. We note that the smallest integrable skip-graph has 4 vertices; therefore this family starts with four vertices. It is an open question whether there are other integrable families of graphs whose smallest member is larger than four vertices and that is not constructed by embedding or cloning. Moreover, it is unclear whether there are other operations beyond cloning and embedding that generate new integrable graphs from integrable graphs. The final hold-out graph in our study suggests either a new family or a new operation that generates integrable

graphs from other integrable graphs. This line of research is similar to the search for structure in the simple groups, and has the potential to quantify deep connections between combinatorial structures and integrable dynamics.

Acknowledgements

M.V. was supported in part by an Erickson Discovery Grant from the Pennsylvania State University. C.G. was supported in part by the National Science Foundation under grant CMMI-1932991.

Data and Code Availability

Mathematica notebooks are provided as supplementary materials and contain the code needed to reproduce the results in this paper.

Appendix A. A Double Embedding

By way of example, we illustrate the conserved quantities generated when two embedded graphs are themselves embedded in a graph with Itoh-style conserved quantities. The graph in question is shown in Fig. A1. As shown in [11], the conserved quantities for

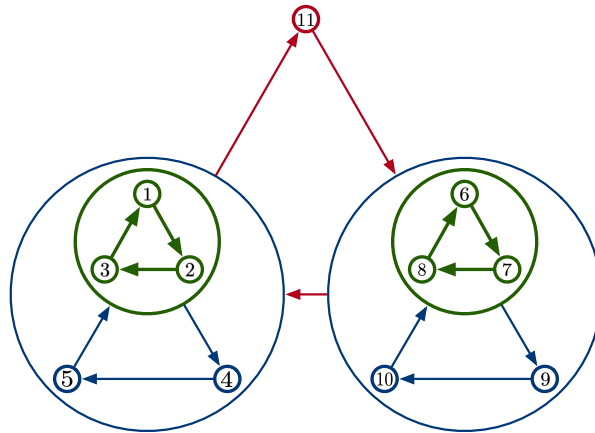


Figure A1. Graphs can be recursively embedded within each other to create new integrable dynamics.

one of the embedded graphs are,

$$H_1 = x_1 + x_2 + x_3 + x_4 + x_5 \quad (\text{A.1})$$

$$H_2 = (x_1 + x_2 + x_3)x_4x_5 \quad (\text{A.2})$$

$$H_3 = x_1x_2x_3x_4^3x_5^3. \quad (\text{A.3})$$

These also follow immediately from Theorem 4.2. Consequently, we can read off ten conserved quantities.

$$\begin{aligned}
H_{10} &= (x_1x_2x_3x_4^3x_5^3)(x_6x_7x_8x_9^3x_{10}^3)x_{11}^9 \\
H_9 &= [(x_1 + x_2 + x_3)x_4x_5]^3 (x_6x_7x_8x_9^3x_{10}^3)x_{11}^9 \\
H_8 &= (x_1x_2x_3x_4^3x_5^3) [(x_6 + x_7 + x_8)x_9x_{10}]^3 x_{11}^9 \\
H_7 &= (x_1 + x_2 + x_3 + x_4 + x_5)^9 (x_6x_7x_8x_9^3x_{10}^3)x_{11}^9 \\
H_6 &= (x_1x_2x_3x_4^3x_5^3)(x_6 + x_7 + x_8 + x_9 + x_{10})^9 x_{11}^9 \\
H_5 &= [(x_1 + x_2 + x_3)x_4x_5] [(x_6 + x_7 + x_8)x_9x_{10}] x_{11}^3 \\
H_4 &= (x_1 + x_2 + x_3 + x_4 + x_5)^3 [(x_6 + x_7 + x_8)x_9x_{10}] x_{11}^3 \\
H_3 &= [(x_1 + x_2 + x_3)x_4x_5] (x_6 + x_7 + x_8 + x_9 + x_{10})^3 x_{11}^3 \\
H_2 &= (x_1 + x_2 + x_3 + x_4 + x_5)(x_6 + x_7 + x_8 + x_9 + x_{10})x_{11} \\
H_1 &= (x_1 + x_2 + x_3 + x_4 + x_5) + (x_6 + x_7 + x_8 + x_9 + x_{10}) + x_{11}
\end{aligned}$$

Computation by hand or using the computational tools included in the SI shows that these quantities commute under the bracket, as expected.

References

- [1] Arnol'd V I 2013 *Mathematical methods of classical mechanics* vol 60 (Springer Science & Business Media)
- [2] Wigner E P 1964 *Proceedings of the National Academy of Sciences* **51** 956–965
- [3] Butterfield J 2006 On symmetry and conserved quantities in classical mechanics *Physical theory and its interpretation: Essays in honor of Jeffrey bub* (Springer) pp 43–100
- [4] Laurent-Gengoux C, Pichereau A and Vanhaecke P 2012 *Poisson structures* vol 347 (Springer Science & Business Media)
- [5] Smale S 1976 *Journal of Mathematical Biology* **3** 5–7
- [6] Itoh Y 1987 *Progress of theoretical physics* **78** 507–510
- [7] Itoh Y 2008 *Journal of Physics A: Mathematical and Theoretical* **42** 025201
- [8] Bogoyavlenskij O, Itoh Y and Yukawa T 2008 *Journal of mathematical physics* **49**
- [9] Evripidou C, Kassotakis P and Vanhaecke P 2021 *Mathematical Physics, Analysis and Geometry* **24** 1–28
- [10] Evripidou C, Kassotakis P and Vanhaecke P 2022 *Journal of Physics A: Mathematical and Theoretical* **55** 325201
- [11] Paik J and Griffin C 2023 *Physical Review E* **107** L052202
- [12] Hofbauer J and Sigmund K 1998 *Evolutionary Games and Population Dynamics* (Cambridge University Press)

- [13] Hofbauer J and Sigmund K 2003 *Bulletin of the American Mathematical Society* **40** 479–519
- [14] Weibull J W 1997 *Evolutionary Game Theory* (MIT Press)
- [15] Tanimoto J 2015 *Fundamentals of evolutionary game theory and its applications* (Springer)
- [16] Tanimoto J 2019 *Evolutionary Games With Sociophysics* (Springer)
- [17] Akin E and Losert V 1984 *Journal of mathematical biology* **20** 231–258
- [18] Allesina S and Levine J M 2011 *Proceedings of the National Academy of Sciences* **108** 5638–5642
- [19] Grilli J, Barabás G, Michalska-Smith M J and Allesina S 2017 *Nature* **548** 210–213
- [20] Miller Z R, Clenet M, Libera K D, Massol F and Allesina S 2023 *bioRxiv* (Preprint <https://www.biorxiv.org/content/early/2023/07/13/2023.03.23.533867.full.pdf>) URL <https://www.biorxiv.org/content/early/2023/07/13/2023.03.23.533867>
- [21] Veselov A P and Shabat A B 1993 *Funktsional’nyi Analiz i ego Prilozheniya* **27** 1–21
- [22] Moser J 2005 *Dynamical Systems, Theory and Applications: Battelle Seattle 1974 Rencontres* 467–497
- [23] Kac M and van Moerbeke P 1975 *Advances in Mathematics* **16** 160–169
- [24] Bogoyavlensky O I 1988 *Physics Letters A* **134** 34–38
- [25] Charalambides S A, Damianou P A and Evripidou C A 2015 Generalized lotka—volterra systems connected with simple lie algebras *Journal of Physics: Conference Series* vol 621 (IOP Publishing) p 012004
- [26] Damianou P A, Evripidou C A, Kassotakis P and Vanhaecke P 2017 *Journal of Mathematical Physics* **58**
- [27] Parmelee C, Moore S, Morrison K and Curto C 2022 *PloS one* **17** e0264456
- [28] Parmelee C, Alvarez J L, Curto C and Morrison K 2022 *SIAM journal on applied dynamical systems* **21** 1597–1630
- [29] Griffin C 2021 *Chaos, Solitons & Fractals* **153** 111508
- [30] Ovsienko V, Schwartz R E and Tabachnikov S 2013 *Duke Mathematical Journal* **162** 2149 – 2196 URL <https://doi.org/10.1215/00127094-2348219>
- [31] Marsden J E and Ratiu T S 2013 *Introduction to mechanics and symmetry: a basic exposition of classical mechanical systems* vol 17 (Springer Science & Business Media)
- [32] Hofbauer J 1996 *Journal of mathematical biology* **34** 675–688
- [33] Bogoyavlenskii O I 1991 *Russian Mathematical Surveys* **46** 1
- [34] McKay B 2024 Digraphs <https://users.cecs.anu.edu.au/~bdm/data/digraphs.html>

- [35] Griffin C H 2023 *Applied Graph Theory: An Introduction with Graph Optimization and Algebraic Graph Theory* (World Scientific)
- [36] Wolf A, Swift J B, Swinney H L and Vastano J A 1985 *Physica D: nonlinear phenomena* **16** 285–317
- [37] Sandri M 1996 *Mathematica Journal* **6** 78–84
- [38] Griffin C, Semonsen J and Belmonte A 2022 *Physica A: Statistical Mechanics and its Applications* **597** 127281